

Handbook of Robotics

Chapter 1: Kinematics

Ken Waldron
Department of Mechanical Engineering
Stanford University
Stanford, CA 94305, USA

Jim Schmiedeler
Department of Mechanical Engineering
The Ohio State University
Columbus, OH 43210, USA

September 17, 2007

Contents

1	Kinematics	1
1.1	Introduction	1
1.2	Position and Orientation Representation	1
1.2.1	Position and Displacement	2
1.2.2	Orientation and Rotation	2
	Rotation Matrices	2
	Euler Angles	3
	Fixed Angles	3
	Angle-Axis	4
	Quaternions	4
1.2.3	Homogeneous Transformations	5
1.2.4	Screw Transformations	5
	Chasles' Theorem	6
	Rodrigues' Equation	7
1.2.5	Matrix Exponential Parameterization	8
	Exponential Coordinates for Rotation	8
	Exponential Coordinates for Rigid Body Motion	8
1.2.6	Plücker Coordinates	9
1.3	Joint Kinematics	9
1.3.1	Lower Pair Joints	10
	Revolute	10
	Prismatic	10
	Helical	10
	Cylindrical	11
	Spherical	11
	Planar	12
1.3.2	Higher Pair Joints	12
	Rolling Contact	12
1.3.3	Compound Joints	12
	Universal	12
1.3.4	6-DOF Joint	12
1.3.5	Physical Realization	13
1.3.6	Holonomic and Nonholonomic Constraints	13
1.3.7	Generalized Coordinates	13
1.4	Geometric Representation	13
1.5	Workspace	15
1.6	Forward Kinematics	16
1.7	Inverse Kinematics	16

1.7.1	Closed-Form Solutions	17
	Algebraic Methods	17
	Geometric Methods	17
1.7.2	Numerical Methods	18
	Symbolic Elimination Methods	18
	Continuation Methods	18
	Iterative Methods	18
1.8	Forward Instantaneous Kinematics	18
1.8.1	Jacobian	19
1.9	Inverse Instantaneous Kinematics	19
1.9.1	Inverse Jacobian	19
1.10	Static Wrench Transmission	20
1.11	Conclusions and Further Reading	20

List of Figures

1.1	Initial and final positions of an arbitrary point in a body undergoing a screw displacement. ${}^i\mathbf{r}$ is the position of the point relative to the moving frame, which is coincident with the fixed reference frame j in its initial position. ${}^j\mathbf{r}$ is the position of the point relative to the fixed frame after the screw displacement of the moving body.	7
1.2	Schematic of the numbering of bodies and joints in a robotic manipulator, the convention for attaching reference frames to the bodies, and the definitions of the four parameters, a_i , α_i , d_i , and θ_i , that locate one frame relative to another.	14
1.3	Example six-degree-of-freedom serial chain manipulator composed of an articulated arm with no joint offsets and a spherical wrist.	15

List of Tables

1.1	Equivalent rotation matrices for various representations of orientation, with abbreviations $c_\theta := \cos \theta$, $s_\theta := \sin \theta$, and $v_\theta := 1 - \cos \theta$	3
1.5	Joint model formulas for one-degree-of-freedom lower pair joints, with abbreviations $c_{\theta_i} := \cos \theta_i$ and $s_{\theta_i} := \sin \theta_i$	11
1.2	Conversions from a rotation matrix to various representations of orientation.	21
1.3	Conversions from angle-axis to unit quaternion representations of orientation and vice versa.	21
1.4	Conversions from a screw transformation to a homogeneous transformation and vice versa, with abbreviations $c_\theta := \cos \theta$, $s_\theta := \sin \theta$, and $v_\theta := 1 - \cos \theta$	21
1.7	Geometric parameters of the example serial chain manipulator in Figure 1.3.	22
1.8	Forward kinematics of the example serial chain manipulator in Figure 1.3, with abbreviations $c_{\theta_i} := \cos \theta_i$ and $s_{\theta_i} := \sin \theta_i$	22
1.9	Inverse position kinematics of the articulated arm within the example serial chain manipulator in Figure 1.3.	22
1.10	Inverse orientation kinematics of the spherical wrist within the example serial chain manipulator in Figure 1.3, with abbreviations $c_{\theta_i} := \cos \theta_i$ and $s_{\theta_i} := \sin \theta_i$	22
1.11	Algorithm for computing the columns of the Jacobian from the free modes of the joints.	22
1.6	Joint model formulas for higher-degree-of-freedom lower pair joints, universal joint, rolling contact joint, and 6-DOF joint, with abbreviations $c_{\theta_i} := \cos \theta_i$ and $s_{\theta_i} := \sin \theta_i$. *The Euler angles α_i , β_i , and γ_i could be used in place of the unit quaternion ϵ_i to represent orientation.	23

Chapter 1

Kinematics

Kinematics pertains to the motion of bodies in a robotic mechanism without regard to the forces/torques that cause the motion. Since robotic mechanisms are by their very essence designed for motion, kinematics is the most fundamental aspect of robot design, analysis, control, and simulation. The robotics community has focused on efficiently applying different representations of position and orientation and their derivatives with respect to time to solve foundational kinematics problems.

This chapter will present the most useful representations of the position and orientation of a body in space, the kinematics of the joints most commonly found in robotic mechanisms, and a convenient convention for representing the geometry of robotic mechanisms. These representational tools will be applied to compute the **workspace**, the **forward** and **inverse kinematics**, the **forward** and **inverse instantaneous kinematics**, and the **static wrench transmission** of a robotic mechanism. For brevity, the focus will be on algorithms applicable to open-chain mechanisms.

The goal of this chapter is to provide the reader with general tools in tabulated form and a broader overview of algorithms that can be together applied to solve kinematics problems pertaining to a particular robotic mechanism.

1.1 Introduction

Unless explicitly stated otherwise, robotic mechanisms are systems of rigid bodies connected by joints. The position and orientation of a rigid body in space are collectively termed the “pose”. Therefore, robot kinematics describes the pose, velocity, acceleration, and all higher order derivatives of the pose of the bodies that comprise a mechanism. Since kinematics does not address the forces/torques that induce motion, this chapter focuses on describing pose and velocity. These descriptions

are foundational elements of dynamics (Chapter 2), motion planning (Chapter 5), and motion control (Chapter 6) algorithms.

Among the many possible topologies in which systems of bodies can be connected, two are of particular importance in robotics: serial chains and fully parallel mechanisms. A serial chain is a system of rigid bodies in which each member is connected to two others, except for the first and last members that are each connected to only one other member. A fully parallel mechanism is one in which there are two members that are connected together by multiple joints. In practice, each “joint” is often itself a serial chain. This chapter focuses almost exclusively on algorithms applicable to serial chains. Parallel mechanisms are dealt with in more detail in Chapter 12 Parallel Mechanisms and Robots.

1.2 Position and Orientation Representation

Spatial, rigid body kinematics can be viewed as a comparative study of different ways of representing the pose of a body. Translations and rotations, referred to in combination as rigid body displacements, are also expressed with these representations. No one approach is optimal for all purposes, but the advantages of each can be leveraged appropriately to facilitate the solution of different problems.

The minimum number of coordinates required to locate a body in Euclidean space is six. Many representations of spatial pose employ sets with superabundant coordinates in which auxiliary relationships exist among the coordinates. The number of independent auxiliary relationships is the difference between the number of coordinates in the set and six.

This chapter and those that follow it make frequent

use of “coordinate reference frames” or simply “frames”. A coordinate reference frame i consists of an origin, denoted O_i , and a triad of mutually orthogonal basis vectors, denoted $[\hat{\mathbf{x}}_i \hat{\mathbf{y}}_i \hat{\mathbf{z}}_i]$, that are all fixed within a particular body. The pose of a body will always be expressed relative to some other body, so it can be expressed as the pose of one coordinate frame relative to another. Similarly, rigid body displacements can be expressed as displacements between two coordinate frames, one of which may be referred to as “moving”, while the other may be referred to as “fixed”. This indicates that the observer is located in a stationary position within the fixed reference frame, not that there exists any absolutely fixed frame.

1.2.1 Position and Displacement

The position of the origin of coordinate frame i relative to coordinate frame j can be denoted by the 3×1 vector

$${}^j\mathbf{p}_i = \begin{bmatrix} {}^j p_i^x \\ {}^j p_i^y \\ {}^j p_i^z \end{bmatrix}.$$

The components of this vector are the Cartesian coordinates of O_i in the j frame, which are the projections of the vector ${}^j\mathbf{p}_i$ onto the corresponding axes. The vector components could also be expressed as the spherical or cylindrical coordinates of O_i in the j frame. Such representations have advantages for analysis of robotic mechanisms including spherical and cylindrical joints.

A translation is a displacement in which no point in the rigid body remains in its initial position and all straight lines in the rigid body remain parallel to their initial orientations. (The points and lines are not necessarily contained within the boundaries of the finite rigid body, but rather, any point or line in space can be taken to be rigidly fixed in a body.) The translation of a body in space can be represented by the combination of its positions prior to and following the translation. Conversely, the position of a body can be represented as a translation that takes the body from a position in which the coordinate frame fixed to the body coincides with the fixed coordinate frame to the current position in which the two frames are not coincident. Thus, any representation of position can be used to create a representation of displacement, and vice-versa.

1.2.2 Orientation and Rotation

There is significantly greater breadth in the representation of orientation than in that of position. This section

does not include an exhaustive summary, but focuses on the representations most commonly applied to robotic mechanisms.

A rotation is a displacement in which at least one point of the rigid body remains in its initial position and not all lines in the body remain parallel to their initial orientations. For example, a body in a circular orbit rotates about an axis through the center of its circular path, and every point on the axis of rotation is a point in the body that remains in its initial position. As in the case of position and translation, any representation of orientation can be used to create a representation of rotation, and vice-versa.

Rotation Matrices

The orientation of coordinate frame i relative to coordinate frame j can be denoted by expressing the basis vectors $[\hat{\mathbf{x}}_i \hat{\mathbf{y}}_i \hat{\mathbf{z}}_i]$ in terms of the basis vectors $[\hat{\mathbf{x}}_j \hat{\mathbf{y}}_j \hat{\mathbf{z}}_j]$. This yields $[{}^j\hat{\mathbf{x}}_i \ {}^j\hat{\mathbf{y}}_i \ {}^j\hat{\mathbf{z}}_i]$, which when written together as a 3×3 matrix is known as the rotation matrix. The components of ${}^j\mathbf{R}_i$ are the dot products of basis vectors of the two coordinate frames.

$${}^j\mathbf{R}_i = \begin{bmatrix} \hat{\mathbf{x}}_i \cdot \hat{\mathbf{x}}_j & \hat{\mathbf{y}}_i \cdot \hat{\mathbf{x}}_j & \hat{\mathbf{z}}_i \cdot \hat{\mathbf{x}}_j \\ \hat{\mathbf{x}}_i \cdot \hat{\mathbf{y}}_j & \hat{\mathbf{y}}_i \cdot \hat{\mathbf{y}}_j & \hat{\mathbf{z}}_i \cdot \hat{\mathbf{y}}_j \\ \hat{\mathbf{x}}_i \cdot \hat{\mathbf{z}}_j & \hat{\mathbf{y}}_i \cdot \hat{\mathbf{z}}_j & \hat{\mathbf{z}}_i \cdot \hat{\mathbf{z}}_j \end{bmatrix} \quad (1.1)$$

Because the basis vectors are unit vectors and the dot product of any two unit vectors is the cosine of the angle between them, the components are commonly referred to as direction cosines.

An elementary rotation of frame i about the $\hat{\mathbf{z}}_j$ axis through an angle θ is

$$\mathbf{R}_Z(\theta) = \begin{bmatrix} \cos \theta & -\sin \theta & 0 \\ \sin \theta & \cos \theta & 0 \\ 0 & 0 & 1 \end{bmatrix}, \quad (1.2)$$

while the same rotation about the $\hat{\mathbf{y}}_j$ axis is

$$\mathbf{R}_Y(\theta) = \begin{bmatrix} \cos \theta & 0 & \sin \theta \\ 0 & 1 & 0 \\ -\sin \theta & 0 & \cos \theta \end{bmatrix}, \quad (1.3)$$

and about the $\hat{\mathbf{x}}_j$ axis is

$$\mathbf{R}_X(\theta) = \begin{bmatrix} 1 & 0 & 0 \\ 0 & \cos \theta & -\sin \theta \\ 0 & \sin \theta & \cos \theta \end{bmatrix}. \quad (1.4)$$

The rotation matrix ${}^j\mathbf{R}_i$ contains nine elements, while only three parameters are required to define the orientation of a body in space. Therefore, six auxiliary relationships exist between the elements of the matrix. Because

the basis vectors of coordinate frame i are mutually orthonormal, as are the basis vectors of coordinate frame j , the columns of ${}^j\mathbf{R}_i$ formed from the dot products of these vectors are also mutually orthonormal. A matrix composed of mutually orthonormal vectors is known as an orthogonal matrix and has the property that its inverse is simply its transpose. This property provides the six auxiliary relationships. Three require the column vectors to have unit length, and three require the column vectors to be mutually orthogonal. Alternatively, the orthogonality of the rotation matrix can be seen by considering the frames in reverse order. The orientation of coordinate frame j relative to coordinate frame i is the rotation matrix ${}^i\mathbf{R}_j$ whose rows are clearly the columns of the matrix ${}^j\mathbf{R}_i$. Rotation matrices are combined through simple matrix multiplication such that the orientation of frame i relative to frame k can be expressed as

$${}^k\mathbf{R}_i = {}^k\mathbf{R}_j {}^j\mathbf{R}_i.$$

In summary, ${}^j\mathbf{R}_i$ is the rotation matrix that transforms a vector expressed in coordinate frame i to a vector expressed in coordinate frame j . It provides a representation of the orientation of frame i relative to j and thus, can be a representation of rotation from frame i to frame j . Table 1.1 lists the equivalent rotation matrices for the other representations of orientation listed in this section. Table 1.2 contains the conversions from a known rotation matrix to these other representations.

Euler Angles

For a minimal representation, the orientation of coordinate frame i relative to coordinate frame j can be denoted as a vector of three angles $[\alpha, \beta, \gamma]$. These angles are known as Euler angles when each represents a rotation about an axis of a moving coordinate frame. In this way, the location of the axis of each successive rotation depends upon the preceding rotation(s), so the order of the rotations must accompany the three angles to define the orientation. For example, the symbols $[\alpha, \beta, \gamma]$ are used throughout this handbook to indicate Z-Y-X Euler angles. Taking the moving frame i and the fixed frame j to be initially coincident, α is the rotation about the \hat{z} axis of frame i , β is the rotation about the rotated \hat{y} axis of frame i , and finally, γ is the rotation about the twice rotated \hat{x} axis of frame i . The equivalent rotation matrix ${}^j\mathbf{R}_i$ is given in Table 1.1. Z-Y-Z and Z-X-Z Euler angles are other commonly used conventions from among the 12 different possible orders of rotations.

Z-Y-X Euler Angles $[\alpha, \beta, \gamma]$:

$${}^j\mathbf{R}_i = \begin{bmatrix} c_\alpha c_\beta & c_\alpha s_\beta s_\gamma - s_\alpha c_\gamma & c_\alpha s_\beta c_\gamma + s_\alpha s_\gamma \\ s_\alpha c_\beta & s_\alpha s_\beta s_\gamma + c_\alpha c_\gamma & s_\alpha s_\beta c_\gamma - c_\alpha s_\gamma \\ -s_\beta & c_\beta s_\gamma & c_\beta c_\gamma \end{bmatrix}$$

X-Y-Z Fixed Angles $[\psi, \theta, \phi]$:

$${}^j\mathbf{R}_i = \begin{bmatrix} c_\phi c_\theta & c_\phi s_\theta s_\psi - s_\phi c_\psi & c_\phi s_\theta c_\psi + s_\phi s_\psi \\ s_\phi c_\theta & s_\phi s_\theta s_\psi + c_\phi c_\psi & s_\phi s_\theta c_\psi - c_\phi s_\psi \\ -s_\theta & c_\theta s_\psi & c_\theta c_\psi \end{bmatrix}$$

Angle-Axis $\theta\hat{w}$:

$${}^j\mathbf{R}_i = \begin{bmatrix} w_x^2 v_\theta + c_\theta & w_x w_y v_\theta - w_z s_\theta & w_x w_z v_\theta + w_y s_\theta \\ w_x w_y v_\theta + w_z s_\theta & w_y^2 v_\theta + c_\theta & w_y w_z v_\theta - w_x s_\theta \\ w_x w_z v_\theta - w_y s_\theta & w_y w_z v_\theta + w_x s_\theta & w_z^2 v_\theta + c_\theta \end{bmatrix}$$

Unit Quaternions $[\epsilon_0 \ \epsilon_1 \ \epsilon_2 \ \epsilon_3]^T$:

$${}^j\mathbf{R}_i = \begin{bmatrix} 1 - 2(\epsilon_2^2 + \epsilon_3^2) & 2(\epsilon_1\epsilon_2 - \epsilon_0\epsilon_3) & 2(\epsilon_1\epsilon_3 + \epsilon_0\epsilon_2) \\ 2(\epsilon_1\epsilon_2 + \epsilon_0\epsilon_3) & 1 - 2(\epsilon_1^2 + \epsilon_3^2) & 2(\epsilon_2\epsilon_3 - \epsilon_0\epsilon_1) \\ 2(\epsilon_1\epsilon_3 - \epsilon_0\epsilon_2) & 2(\epsilon_2\epsilon_3 + \epsilon_0\epsilon_1) & 1 - 2(\epsilon_1^2 + \epsilon_2^2) \end{bmatrix}$$

Table 1.1: Equivalent rotation matrices for various representations of orientation, with abbreviations $c_\theta := \cos \theta$, $s_\theta := \sin \theta$, and $v_\theta := 1 - \cos \theta$.

Regardless of the order of rotations, an Euler angle representation of orientation always exhibits a singularity when the first and last rotations both occur about the same axis. This can be readily seen in Table 1.2 wherein the angles α and γ are undefined when $\beta = \pm 90^\circ$. (For Z-Y-Z and Z-X-Z Euler angles, the singularity occurs when the second rotation is 0° or 180° .) This creates a problem in relating the angular velocity vector of a body to the time derivatives of Euler angles, which somewhat limits their usefulness in modeling robotic systems. This velocity relationship for Z-Y-X Euler angles is

$$\begin{bmatrix} \dot{\alpha} \\ \dot{\beta} \\ \dot{\gamma} \end{bmatrix} = \begin{bmatrix} -\sin \beta & 0 & 1 \\ \cos \beta \sin \gamma & \cos \gamma & 0 \\ \cos \beta \cos \gamma & -\sin \beta & 0 \end{bmatrix} \begin{bmatrix} \omega_x \\ \omega_y \\ \omega_z \end{bmatrix}. \quad (1.5)$$

Fixed Angles

A vector of three angles can also denote the orientation of coordinate frame i relative to coordinate frame j when each angle represents a rotation about an axis of a fixed

reference frame. Appropriately, such angles are referred to as Fixed Angles, and the order of the rotations must again accompany the angles to define the orientation. X-Y-Z Fixed Angles, denoted here as $[\psi, \theta, \phi]$, are a common convention from among the, again, 12 different possible orders of rotations. Taking the moving frame i and the fixed frame j to be initially coincident, ψ is the yaw rotation about the fixed \hat{x}_j axis, θ is the pitch rotation about the fixed \hat{y}_j axis, and ϕ is the roll rotation about the fixed \hat{z}_j axis. As can be seen by comparing the respective equivalent rotation matrices in Table 1.1 and the respective conversions in Table 1.2, a set of X-Y-Z Fixed Angles is exactly equivalent to the same set of Z-Y-X Euler Angles ($\alpha = \phi$, $\beta = \theta$, and $\gamma = \psi$). This result holds in general such that three rotations about the three axes of a fixed frame define the same orientation as the same three rotations taken in the opposite order about the three axes of a moving frame. Likewise, all fixed angle representations of orientations suffer from the singularity discussed for Euler angles. Also, the relationship between the time derivatives of fixed angles and the angular velocity vector is similar to the relationship for Euler angles.

Angle-Axis

A single angle θ in combination with a unit vector \hat{w} can also denote the orientation of coordinate frame i relative to coordinate frame j . In this case, frame i is rotated through the angle θ about an axis defined by the vector $\hat{w} = [w_x \ w_y \ w_z]^T$ relative to frame j . The vector \hat{w} is sometimes referred to as the equivalent axis of a finite rotation. The angle-axis representation, typically written as either $\theta\hat{w}$ or $[\theta w_x \ \theta w_y \ \theta w_z]^T$, is superabundant by one because it contains four parameters. The auxiliary relationship that resolves this is the unit magnitude of vector \hat{w} . Even with this auxiliary relationship, the angle-axis representation is not unique because rotation through an angle of $-\theta$ about $-\hat{w}$ is equivalent to a rotation through θ about \hat{w} . Table 1.3 contains the conversions from angle-axis representation to unit quaternions and vice versa. The conversions from these two representations to Euler angles or fixed angles can be easily found by using the conversions in Table 1.2 in conjunction with the equivalent rotation matrices in Table 1.1. Velocity relationships are more easily dealt with using the closely related quaternion representation.

Quaternions

The quaternion representation of orientation due to Hamilton [18], while largely superseded by the simpler vector representations of Gibbs [61] and Grassmann [17], is extremely useful for problems in robotics that result in representational singularities in the vector/matrix notation [33]. Quaternions do not suffer from singularities as Euler angles do.

A quaternion ϵ is defined to have the form,

$$\epsilon = \epsilon_0 + \epsilon_1 i + \epsilon_2 j + \epsilon_3 k,$$

where the components ϵ_0 , ϵ_1 , ϵ_2 , and ϵ_3 are scalars, sometimes referred to as Euler parameters, and i , j , and k are operators. The operators are defined to satisfy the following combinatory rules:

$$ii = jj = kk = -1$$

$$ij = k, \quad jk = i, \quad ki = j,$$

$$ji = -k, \quad kj = -i, \quad ik = -j.$$

Two quaternions are added by adding the respective components separately, so the operators act as separators. The null element for addition is the quaternion $\mathbf{0} = 0 + 0i + 0j + 0k$, and quaternion sums are associative, commutative, and distributive. The null element for multiplication is $\mathbf{1} = 1 + 0i + 0j + 0k$, as can be seen using $\mathbf{1}\epsilon = \epsilon$ for any quaternion ϵ . Quaternion products are associative and distributive, but not commutative, and following the conventions of the operators and addition, have the form

$$\begin{aligned} \mathbf{ab} = & a_0 b_0 - a_1 b_1 - a_2 b_2 - a_3 b_3 \\ & + (a_0 b_1 + a_1 b_0 + a_2 b_3 - a_3 b_2) i \\ & + (a_0 b_2 + a_2 b_0 + a_3 b_1 - a_1 b_3) j \\ & + (a_0 b_3 + a_3 b_0 + a_1 b_2 - a_2 b_1) k \end{aligned} \quad (1.6)$$

It is convenient to define the conjugate of a quaternion,

$$\tilde{\epsilon} = \epsilon_0 - \epsilon_1 i - \epsilon_2 j - \epsilon_3 k,$$

so that

$$\epsilon\tilde{\epsilon} = \tilde{\epsilon}\epsilon = \epsilon_0^2 + \epsilon_1^2 + \epsilon_2^2 + \epsilon_3^2.$$

A unit quaternion can then be defined such that, $\epsilon\tilde{\epsilon} = 1$. Often, ϵ_0 is referred to as the scalar part of the quaternion, and $[\epsilon_1 \ \epsilon_2 \ \epsilon_3]^T$ is referred to as the vector part.

Unit quaternions are used to describe orientation, and the unit magnitude provides the auxiliary relationship to resolve the use of superabundant (four) coordinates. A vector is defined in quaternion notation as a quaternion

with $\epsilon_0 = 0$. Thus, a vector $\mathbf{p} = [p_x \ p_y \ p_z]^T$ can be expressed as a quaternion $\mathbf{p} = p_x i + p_y j + p_z k$. For any unit quaternion ϵ , the operation $\epsilon \mathbf{p} \bar{\epsilon}$ performs a rotation of the vector \mathbf{p} about the direction $[\epsilon_1 \ \epsilon_2 \ \epsilon_3]^T$. This is clearly seen by expanding the operation $\epsilon \mathbf{p} \bar{\epsilon}$ and comparing the results with the equivalent rotation matrix listed in Table 1.1. Also, as shown in Table 1.3, unit quaternions are closely related to the angle-axis representation of orientation. ϵ_0 corresponds to the angle of rotation, while ϵ_1 , ϵ_2 , and ϵ_3 define the axis of rotation.

For velocity analysis, the time derivative of the quaternion can be related to the angular velocity vector as

$$\begin{bmatrix} \dot{\epsilon}_0 \\ \dot{\epsilon}_1 \\ \dot{\epsilon}_2 \\ \dot{\epsilon}_3 \end{bmatrix} = \frac{1}{2} \begin{bmatrix} -\epsilon_1 & -\epsilon_2 & -\epsilon_3 \\ \epsilon_0 & \epsilon_3 & -\epsilon_2 \\ -\epsilon_3 & \epsilon_0 & \epsilon_1 \\ \epsilon_2 & -\epsilon_1 & \epsilon_0 \end{bmatrix} \begin{bmatrix} \omega_x \\ \omega_y \\ \omega_z \end{bmatrix}. \quad (1.7)$$

While a unit quaternion represents only the orientation of a body, quaternions may be dualized [10, 23, 49] to create an algebra that provides a description of the position and orientation of a body in space. Other combined representations are discussed in the following sections.

1.2.3 Homogeneous Transformations

The preceding sections have addressed representations of position and orientation separately. With homogeneous transformations, position vectors and rotation matrices are combined together in a compact notation. Any vector ${}^i \mathbf{r}$ expressed relative to the i coordinate frame can be expressed relative to the j coordinate frame if the position and orientation of the i frame are known relative to the j frame. Using the notation of Section 1.2.1, the position of the origin of coordinate frame i relative to coordinate frame j can be denoted by the vector ${}^j \mathbf{p}_i = [{}^j p_i^x \ {}^j p_i^y \ {}^j p_i^z]^T$. Using the notation of Section 1.2.2, the orientation of frame i relative to frame j can be denoted by the rotation matrix ${}^j \mathbf{R}_i$. Thus,

$${}^j \mathbf{r} = {}^j \mathbf{R}_i {}^i \mathbf{r} + {}^j \mathbf{p}_i. \quad (1.8)$$

This equation can be written

$$\begin{bmatrix} {}^j \mathbf{r} \\ 1 \end{bmatrix} = \begin{bmatrix} {}^j \mathbf{R}_i & {}^j \mathbf{p}_i \\ \mathbf{0}^T & 1 \end{bmatrix} \begin{bmatrix} {}^i \mathbf{r} \\ 1 \end{bmatrix}, \quad (1.9)$$

where

$${}^j \mathbf{T}_i = \begin{bmatrix} {}^j \mathbf{R}_i & {}^j \mathbf{p}_i \\ \mathbf{0}^T & 1 \end{bmatrix} \quad (1.10)$$

is the 4×4 homogeneous transform matrix and $[{}^j \mathbf{r} \ 1]^T$ and $[{}^i \mathbf{r} \ 1]^T$ are the homogeneous representations of the

position vectors ${}^j \mathbf{r}$ and ${}^i \mathbf{r}$. The matrix ${}^j \mathbf{T}_i$ transforms vectors from coordinate frame i to coordinate frame j . Its inverse ${}^j \mathbf{T}_i^{-1}$ transforms vectors from coordinate frame j to coordinate frame i .

$${}^j \mathbf{T}_i^{-1} = {}^i \mathbf{T}_j = \begin{bmatrix} {}^j \mathbf{R}_i^T & -{}^j \mathbf{R}_i^T {}^j \mathbf{p}_i \\ \mathbf{0}^T & 1 \end{bmatrix}. \quad (1.11)$$

Composition of 4×4 homogeneous transform matrices is accomplished through simple matrix multiplication, just as in the case of 3×3 rotation matrices. Therefore, ${}^k \mathbf{T}_i = {}^k \mathbf{T}_j {}^j \mathbf{T}_i$. Since matrix multiplications do not commute, the order or sequence is important.

The homogeneous transform of a simple rotation about an axis is sometimes denoted **Rot** such that a rotation of θ about an axis $\hat{\mathbf{z}}$ is

$$\mathbf{Rot}(\hat{\mathbf{z}}, \theta) = \begin{bmatrix} \cos \theta & -\sin \theta & 0 & 0 \\ \sin \theta & \cos \theta & 0 & 0 \\ 0 & 0 & 1 & 0 \\ 0 & 0 & 0 & 1 \end{bmatrix}. \quad (1.12)$$

Similarly, the homogeneous transform of a simple translation along an axis is sometimes denoted **Trans** such that a translation of d along an axis $\hat{\mathbf{x}}$ is

$$\mathbf{Trans}(\hat{\mathbf{x}}, d) = \begin{bmatrix} 1 & 0 & 0 & d \\ 0 & 1 & 0 & 0 \\ 0 & 0 & 1 & 0 \\ 0 & 0 & 0 & 1 \end{bmatrix}. \quad (1.13)$$

Homogeneous transformations are particularly attractive when compact notation is desired and/or when ease of programming is the most important consideration. This is not, however, a computationally efficient representation since it introduces a large number of additional multiplications by ones and zeros. Although homogeneous transform matrices technically contain sixteen elements, four are defined to be zero or one, and the remaining elements are composed of a rotation matrix and a position vector. Therefore, the only truly superabundant coordinates come from the rotation matrix component, so the relevant auxiliary relationships are those associated with the rotation matrix.

1.2.4 Screw Transformations

The transformation in Equation 1.8 can be viewed as composed of a rotation between coordinate frames i and j and a separate displacement between those frames. To get from frame i to frame j , one could perform the rotation first, followed by the displacement, or vice versa. Alternatively, the spatial displacement between the frames

can be expressed, except in the case of a pure translation, as a rotation about a unique line combined with a translation parallel to that line.

Chasles' Theorem

Chasles' theorem, in the form stated by Chirikjian and Kyatkin [9], has two parts. The first states that: *Any displacement of a body in space can be accomplished by means of a translation of a designated point from its initial to its final position, followed by a rotation of the whole body about that point to bring it into its final orientation.* The second part states that: *Any displacement of a body in space can be accomplished by means of a rotation of the body about a unique line in space accompanied by a translation of the body parallel to that line.* Such a line is called a screw axis, and it is this second result that is usually thought of as Chasles' theorem.

The first part of the theorem is almost axiomatic. A designated point in a body anywhere in Euclidean space can be displaced from a given initial position to a given final position. By further requiring that all points in the body traverse the same displacement, the body translates so that the designated point moves from its initial position to its final position. The body can then be rotated about that point into any given final orientation.

The second part of the theorem depends on this representation of a spatial displacement and requires a more complex argument. A preliminary theorem due to Euler allows greater specificity about the rotation of the body: *Any displacement of a body in which one point remains fixed is equivalent to a rotation of that body about a unique axis passing through that point.* Geometrically, embedding three points in the moving body and letting one be the fixed point about which rotation occurs, each of the other two will have initial and final positions. The right bisector planes of the lines joining the initial and final positions in each case necessarily contain the fixed point. Any line in the bisector plane can be the axis of a rotation that carries the corresponding point from its initial to its final position. Therefore, the unique line common to the two bisector planes is such that rotation about it will carry any point in the body from its initial to its final position. The rigidity condition requires that all planes in the body that contain that line rotate through the same angle.

For any rotation of a rigid body described by a rotation matrix ${}^j\mathbf{R}_i$, Euler's theorem states that there is an unique eigenvector $\hat{\mathbf{w}}$ such that

$${}^j\mathbf{R}_i\hat{\mathbf{w}} = \hat{\mathbf{w}}, \quad (1.14)$$

where $\hat{\mathbf{w}}$ is a unit vector parallel to the axis of rotation. This expression requires a unit eigenvalue of ${}^j\mathbf{R}_i$ corresponding to the eigenvector $\hat{\mathbf{w}}$. The remaining two eigenvalues are $\cos\theta \pm i\sin\theta$, where i is the complex operator and θ is the angle of rotation of the body about the axis.

Combining the first part of Chasles' theorem with Euler's theorem, a general spatial displacement can be expressed as a translation taking a point from its initial to its final position, followed by a unique rotation about a unique axis through that point that carries the body from its initial to its final orientation. Resolving the translation into components in the direction of and orthogonal to the rotation axis, every point in the body has the same displacement component in the direction of the axis because rotation about it does not affect that component. Projected into a plane normal to the rotation axis, the kinematic geometry of the displacement is identical to that of planar motion. Just as there is a unique point in the plane about which a body could be rotated between two given positions, there is a unique point in the projection plane. If the rotation axis is moved to pass through that point, the spatial displacement can be accomplished by a rotation about that axis combined with a translation along it, as stated by the theorem.

The line about which rotation takes place is called the screw axis of the displacement. The ratio of the linear displacement d to the rotation θ is referred to as the pitch h of the screw axis [33]. Thus,

$$d = h\theta. \quad (1.15)$$

The screw axis of a pure translation is not unique. Any line parallel to the translation can be regarded as the screw axis, and since the rotation θ is zero, the axis of a translation is said to have infinite pitch.

A screw axis is most conveniently represented in any reference frame by means of a unit vector $\hat{\mathbf{w}}$ parallel to it and the position vector $\boldsymbol{\rho}$ of any point lying on it. Additional specification of the pitch h and the angle of rotation θ completely defines the location of a second coordinate frame relative to the reference frame. Thus, a total of eight coordinates define a screw transformation, which is superabundant by two. The unit magnitude of vector $\hat{\mathbf{w}}$ provides one auxiliary relationship, but in general, there is no second auxiliary relationship because the same screw axis is defined by all points lying on it, which is to say that the vector $\boldsymbol{\rho}$ contains one free coordinate.

Algebraically, a screw displacement is represented by

$${}^j\mathbf{r} = {}^j\mathbf{R}_i({}^i\mathbf{r} - \boldsymbol{\rho}) + d\hat{\mathbf{w}} + \boldsymbol{\rho}, \quad (1.16)$$

Comparing this expression to Eq. 1.8 yields

$${}^j\mathbf{p}_i = d\hat{\mathbf{w}} + (\mathbf{1}_{3\times 3} - {}^j\mathbf{R}_i)\boldsymbol{\rho}. \quad (1.17)$$

An expression for d is easily obtained by taking the inner product of both sides of the equation with $\hat{\mathbf{w}}$:

$$d = \hat{\mathbf{w}}^T {}^j\mathbf{p}_i. \quad (1.18)$$

The matrix $\mathbf{1}_{3\times 3} - {}^j\mathbf{R}_i$ is singular, so Eq. 1.17 cannot be solved to give a unique value of $\boldsymbol{\rho}$, but since $\boldsymbol{\rho}$ can represent any point on the screw axis, this would not be appropriate. One component of $\boldsymbol{\rho}$ can be arbitrarily chosen, and any two of the component equations can then be solved to find the two other components of $\boldsymbol{\rho}$. All other points on the screw axis are then given by $\boldsymbol{\rho} + k\hat{\mathbf{w}}$, where k can take any value.

Table 1.4 contains the conversions between screw transformations and homogeneous transformations. Note that the equivalent rotation matrix for a screw transformation has the same form as the equivalent rotation matrix for an angle-axis representation of orientation in Table 1.1. Also, the auxiliary relationship that the vector $\boldsymbol{\rho}$ be orthogonal to the screw axis ($\hat{\mathbf{w}}^T \boldsymbol{\rho} = 0$) is used in Table 1.4 to provide a unique conversion to the screw transformation. The inverse result, that of finding the rotation matrix ${}^j\mathbf{R}_i$ and the translation ${}^j\mathbf{p}_i$ corresponding to a given screw displacement is found from Rodrigues' equation.

Rodrigues' Equation

Given a screw axis, the angular displacement of a body about it, and the translation of the body along it, the displacement of an arbitrary point in that body can be found. Viewing a matrix transformation as describing the displacement of the body, this is equivalent to finding the matrix transformation equivalent to a given screw displacement.

Referring to Figure 1.1, the position vectors of a point before and after a screw displacement can be related

$${}^j\mathbf{r} = \begin{aligned} & {}^i\mathbf{r} + d\hat{\mathbf{w}} + \sin\theta\hat{\mathbf{w}} \times ({}^i\mathbf{r} - \boldsymbol{\rho}) \\ & - (1 - \cos\theta)({}^i\mathbf{r} - \boldsymbol{\rho}) - ({}^i\mathbf{r} - \boldsymbol{\rho}) \cdot \hat{\mathbf{w}}\hat{\mathbf{w}}, \end{aligned} \quad (1.19)$$

where ${}^i\mathbf{r}$ and ${}^j\mathbf{r}$ denote the initial and final positions of the point, $\hat{\mathbf{w}}$ and $\boldsymbol{\rho}$ specify the screw axis, and θ and d give the displacement about it. This result is usually referred to as Rodrigues' Equation [5], which can be written as a matrix transformation [2],

$${}^j\mathbf{r} = {}^j\mathbf{R}_i {}^i\mathbf{r} + {}^j\mathbf{p}_i, \quad (1.20)$$

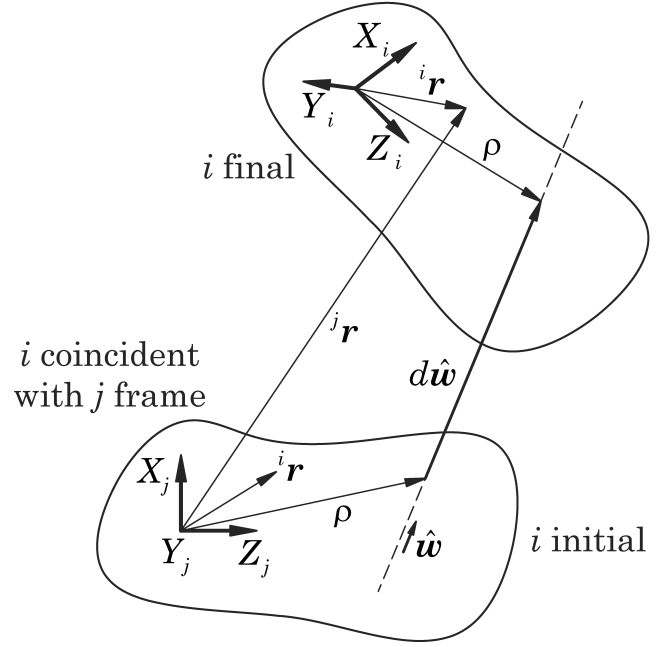


Figure 1.1: Initial and final positions of an arbitrary point in a body undergoing a screw displacement. ${}^i\mathbf{r}$ is the position of the point relative to the moving frame, which is coincident with the fixed reference frame j in its initial position. ${}^j\mathbf{r}$ is the position of the point relative to the fixed frame after the screw displacement of the moving body.

since, when expanded, it gives three linear equations for the components of ${}^j\mathbf{r}$ in terms of those of ${}^i\mathbf{r}$.

$${}^j\mathbf{R}_i = \begin{bmatrix} w_x^2 v_\theta + c_\theta & w_x w_y v_\theta - w_z s_\theta & w_x w_z v_\theta + w_y s_\theta \\ w_x w_y v_\theta + w_z s_\theta & w_y^2 v_\theta + c_\theta & w_y w_z v_\theta - w_x s_\theta \\ w_x w_z v_\theta - w_y s_\theta & w_y w_z v_\theta + w_x s_\theta & w_z^2 v_\theta + c_\theta \end{bmatrix}$$

$${}^j\mathbf{p}_i = (\mathbf{1}_{3\times 3} - {}^j\mathbf{R}_i)\boldsymbol{\rho} + h\theta\hat{\mathbf{w}},$$

where the abbreviations are $c_\theta := \cos\theta$, $s_\theta := \sin\theta$, and $v_\theta = 1 - \cos\theta$. The rotation matrix ${}^j\mathbf{R}_i$ expressed in this form is also called the screw matrix, and these equations give the elements of ${}^j\mathbf{R}_i$ and ${}^j\mathbf{p}_i$ in terms of the screw parameters.

An exception arises in the case of a pure translation, for which $\theta = 0$ and Rodrigues' equation becomes

$${}^j\mathbf{r} = {}^i\mathbf{r} + d\hat{\mathbf{w}}. \quad (1.21)$$

Substituting for this case, ${}^j\mathbf{R}_i = \mathbf{1}_{3\times 3}$ and ${}^j\mathbf{p}_i = d\hat{\mathbf{w}}$.

Additional information on screw theory can be found in [4, 12, 19, 41, 42].

1.2.5 Matrix Exponential Parameterization

The position and orientation of a body can also be expressed in a unified fashion with an exponential mapping. This approach is introduced first with its application to pure rotation and expanded to rigid body motion. More details on the approach can be found in [8] and [34].

Exponential Coordinates for Rotation

The set of all orthogonal matrices with determinant 1, which is the set of all rotation matrices \mathbf{R} , is a *group* under the operation of matrix multiplication denoted as $SO(3) \subset \mathbb{R}^{3 \times 3}$. This stands for *special orthogonal* wherein “special” alludes to the $\det \mathbf{R}$ being +1 instead of ± 1 . The set of rotation matrices satisfies the four axioms of a group:

- *Closure:* $\mathbf{R}_1 \mathbf{R}_2 \in SO(3) \forall \mathbf{R}_1, \mathbf{R}_2 \in SO(3)$;
- *Identity:* $\mathbf{1}_{3 \times 3} \mathbf{R} = \mathbf{R} \mathbf{1}_{3 \times 3} = \mathbf{R} \forall \mathbf{R} \in SO(3)$;
- *Inverse:* $\mathbf{R}^T \in SO(3)$ is the unique inverse of $\mathbf{R} \forall \mathbf{R} \in SO(3)$;
- *Associativity:* $(\mathbf{R}_1 \mathbf{R}_2) \mathbf{R}_3 = \mathbf{R}_1 (\mathbf{R}_2 \mathbf{R}_3) \forall \mathbf{R}_1, \mathbf{R}_2, \mathbf{R}_3 \in SO(3)$.

In the angle-axis representation presented in Section 1.2.2, orientation is expressed as an angle θ of rotation about an axis defined by the unit vector $\hat{\mathbf{w}}$. The equivalent rotation matrix found in Table 1.1 can be expressed as the exponential map

$$\mathbf{R} = e^{S(\hat{\mathbf{w}})\theta} = \mathbf{1}_{3 \times 3} + \theta S(\hat{\mathbf{w}}) + \frac{\theta^2}{2!} S(\hat{\mathbf{w}})^2 + \frac{\theta^3}{3!} S(\hat{\mathbf{w}})^3 + \dots, \quad (1.22)$$

where $S(\hat{\mathbf{w}})$ is the unit skew-symmetric matrix

$$S(\hat{\mathbf{w}}) = \begin{bmatrix} 0 & -w_z & w_y \\ w_z & 0 & -w_x \\ -w_y & w_x & 0 \end{bmatrix}. \quad (1.23)$$

Thus, the exponential map transforms a skew-symmetric matrix $S(\hat{\mathbf{w}})$ that corresponds to an axis of rotation $\hat{\mathbf{w}}$ into an orthogonal matrix \mathbf{R} that corresponds to a rotation about the axis $\hat{\mathbf{w}}$ through an angle of θ . It can be shown that the closed form expression for $e^{S(\hat{\mathbf{w}})\theta}$, which can be efficiently computed, is

$$e^{S(\hat{\mathbf{w}})\theta} = \mathbf{1}_{3 \times 3} + S(\hat{\mathbf{w}}) \sin \theta + S(\hat{\mathbf{w}})^2 (1 - \cos \theta). \quad (1.24)$$

The components of $[\theta w_x \ \theta w_y \ \theta w_z]^T$, which are related to the elements of the rotation matrix \mathbf{R} in Table 1.2, are referred to as the *exponential coordinates* for \mathbf{R} .

Exponential Coordinates for Rigid Body Motion

As indicated in Section 1.2.3, the position and orientation of a body can be expressed by the combination of a position vector $\mathbf{p} \in \mathbb{R}^3$ and a rotation matrix $\mathbf{R} \in SO(3)$. The product space of \mathbb{R}^3 with $SO(3)$ is the group known as $SE(3)$, which stands for *special Euclidean*.

$$SE(3) = \{(\mathbf{p}, \mathbf{R}) : \mathbf{p} \in \mathbb{R}^3, \mathbf{R} \in SO(3)\} = \mathbb{R}^3 \times SO(3).$$

The set of homogeneous transformations satisfies the four axioms of a group:

- *Closure:* $\mathbf{T}_1 \mathbf{T}_2 \in SE(3) \forall \mathbf{T}_1, \mathbf{T}_2 \in SE(3)$;
- *Identity:* $\mathbf{1}_{4 \times 4} \mathbf{T} = \mathbf{T} \mathbf{1}_{4 \times 4} = \mathbf{T} \forall \mathbf{T} \in SE(3)$;
- *Inverse:* the unique inverse of $\mathbf{T} \forall \mathbf{T} \in SE(3)$ is given in Eq. 1.11;
- *Associativity:* $(\mathbf{T}_1 \mathbf{T}_2) \mathbf{T}_3 = \mathbf{T}_1 (\mathbf{T}_2 \mathbf{T}_3) \forall \mathbf{T}_1, \mathbf{T}_2, \mathbf{T}_3 \in SE(3)$.

In the screw transformation representation in Section 1.2.4, position and orientation are expressed by the angle θ of rotation about a screw axis defined by the unit vector $\hat{\mathbf{w}}$, the point $\boldsymbol{\rho}$ on the axis such that $\hat{\mathbf{w}}^T \boldsymbol{\rho} = 0$, and the pitch h of the screw axis. The equivalent homogeneous transformation found in Table 1.4 can be expressed as the exponential map

$$\mathbf{T} = e^{\hat{\boldsymbol{\xi}}\theta} = \mathbf{1}_{4 \times 4} + \hat{\boldsymbol{\xi}}\theta + \frac{(\hat{\boldsymbol{\xi}}\theta)^2}{2!} + \frac{(\hat{\boldsymbol{\xi}}\theta)^3}{3!} + \dots, \quad (1.25)$$

where

$$\hat{\boldsymbol{\xi}} = \begin{bmatrix} S(\hat{\mathbf{w}}) & \mathbf{v} \\ \mathbf{0}^T & 0 \end{bmatrix} \quad (1.26)$$

is the generalization of the unit skew symmetric matrix $S(\hat{\mathbf{w}})$ known as a *twist*. The twist coordinates of $\hat{\boldsymbol{\xi}}$ are given by $\boldsymbol{\xi} := [\hat{\mathbf{w}}^T \mathbf{v}^T]^T$. It can be shown that the closed form expression for $e^{\hat{\boldsymbol{\xi}}\theta}$ is

$$e^{\hat{\boldsymbol{\xi}}\theta} = \begin{bmatrix} e^{S(\hat{\mathbf{w}})\theta} & (\mathbf{1}_{3 \times 3} - e^{S(\hat{\mathbf{w}})\theta})(\hat{\mathbf{w}} \times \mathbf{v}) + \hat{\mathbf{w}}^T \mathbf{v} \theta \hat{\mathbf{w}} \\ \mathbf{0}^T & 1 \end{bmatrix}. \quad (1.27)$$

Comparison of this result with the conversion between homogeneous and screw transformations in Table 1.4 yields

$$\mathbf{v} = \boldsymbol{\rho} \times \hat{\mathbf{w}} \quad (1.28)$$

and

$$h = \hat{\mathbf{w}}^T \mathbf{v}. \quad (1.29)$$

Thus, the exponential map for a twist transforms the initial pose of a body into its final pose. It gives the relative

rigid body motion. The vector $\xi\theta$ contains the *exponential coordinates* for the rigid body transformation.

As for screw transformations, the case of pure translation is unique. In this case, $\dot{\mathbf{w}} = \mathbf{0}$, so

$$e^{\xi\theta} = \begin{bmatrix} \mathbf{1}_{3 \times 3} & \theta \mathbf{v} \\ \mathbf{0}^T & 1 \end{bmatrix}. \quad (1.30)$$

1.2.6 Plücker Coordinates

A minimum of four coordinates are needed to define a line in space. The Plücker coordinates of a line form a six-dimensional vector, so they are superabundant by two. They can be viewed as a pair of three-dimensional vectors; one is parallel to the line, and the other is the “moment” of that vector about the origin. Thus, if \mathbf{u} is any vector parallel to the line and $\boldsymbol{\rho}$ is the position of any point on the line relative to the origin, the Plücker coordinates (L, M, N, P, Q, R) are given by:

$$(L, M, N) = \mathbf{u}^T; (P, Q, R) = (\boldsymbol{\rho} \times \mathbf{u})^T. \quad (1.31)$$

For simply defining a line, the magnitude of \mathbf{u} is not unique, nor is the component of $\boldsymbol{\rho}$ parallel to \mathbf{u} . Two auxiliary relationships are imposed to reduce the set to just four independent coordinates. One is that the scalar product of the two three-dimensional vectors is identically zero.

$$LP + MQ + NR \equiv 0. \quad (1.32)$$

The other is the invariance of the line designated when the coordinates are all multiplied by the same scaling factor.

$$(L, M, N, P, Q, R) \equiv (kL, kM, kN, kP, kQ, kR). \quad (1.33)$$

This relationship may take the form of constraining \mathbf{u} to have unit magnitude so that L , M , and N are the direction cosines.

In this handbook, it is often useful to express velocities in Plücker coordinates, wherein unlike the definition of lines, the magnitudes of the the two three-dimensional vectors are not arbitrary. This leads to the motor notation of Von Mises [3] and Everett [15]. For instantaneously coincident coordinate frames, one fixed and the other embedded in the moving body, $\boldsymbol{\omega}$ is the angular velocity of the body and \mathbf{v}_O is the velocity of the origin O of the body-fixed frame when both are expressed relative to the fixed frame. This provides a Plücker coordinate system for the spatial velocity \mathbf{v} of the body. The Plücker coordinates of \mathbf{v} are simply the Cartesian

coordinates of $\boldsymbol{\omega}$ and \mathbf{v}_O ,

$$\mathbf{v} = \begin{bmatrix} \boldsymbol{\omega} \\ \mathbf{v} \end{bmatrix}. \quad (1.34)$$

The transformation from Plücker coordinate system i to Plücker coordinate system j for spatial velocities is achieved with the spatial transform ${}^j\mathbf{X}_i$. If \mathbf{v}_i and \mathbf{v}_j denote the spatial velocities of a body relative to the i and j frame, respectively, and ${}^j\mathbf{p}_i$ and ${}^j\mathbf{R}_i$ denote the position and orientation of frame i relative to frame j ,

$$\mathbf{v}_j = {}^j\mathbf{X}_i \mathbf{v}_i, \quad (1.35)$$

where

$${}^j\mathbf{X}_i = \begin{bmatrix} {}^j\mathbf{R}_i & \mathbf{0}_{3 \times 3} \\ S({}^j\mathbf{p}_i) {}^j\mathbf{R}_i & {}^j\mathbf{R}_i \end{bmatrix}, \quad (1.36)$$

such that

$${}^j\mathbf{X}_i^{-1} = {}^i\mathbf{X}_j = \begin{bmatrix} {}^i\mathbf{R}_j & \mathbf{0}_{3 \times 3} \\ -{}^i\mathbf{R}_j S({}^j\mathbf{p}_i) & {}^i\mathbf{R}_j \end{bmatrix} \quad (1.37)$$

and

$${}^k\mathbf{X}_i = {}^k\mathbf{X}_j {}^j\mathbf{X}_i, \quad (1.38)$$

and $S({}^j\mathbf{p}_i)$ is the skew symmetric matrix

$$\begin{bmatrix} 0 & -{}^j p_i^z & {}^j p_i^y \\ {}^j p_i^z & 0 & -{}^j p_i^x \\ -{}^j p_i^y & {}^j p_i^x & 0 \end{bmatrix} \quad (1.39)$$

Spatial vector notation, which includes the spatial velocities and transforms briefly mentioned here, is treated in greater depth in Section 2.2. Specifically, Table 2.1 gives a computationally efficient algorithm for applying a spatial transform.

1.3 Joint Kinematics

Unless explicitly stated otherwise, the kinematic description of robotic mechanisms typically employs a number of idealizations. The links that compose the robotic mechanism are assumed to be perfectly rigid bodies having surfaces that are geometrically perfect in both position and shape. Accordingly, these rigid bodies are connected together at joints where their idealized surfaces are in ideal contact without any clearance between them. The respective geometries of these surfaces in contact determine the freedom of motion between the two links, or the *joint kinematics*.

A kinematic joint is a connection between two bodies that constrains their relative motion. Two bodies that

are in contact with one another create a simple kinematic joint. The surfaces of the two bodies that are in contact are able to move over one another, thereby permitting relative motion of the two bodies. Simple kinematic joints are classified as lower pair joints if contact occurs over surfaces [45] and as higher pair joints if contact occurs only at points or along lines.

A joint model describes the motion of a frame fixed in one body of a joint relative to a frame fixed in the other body. The motion is expressed as a function of the joint's motion variables, and other elements of a joint model include the joint transform, free modes, and constrained modes. The joint transform enables the transformation from the frame in the predecessor body to the frame in the successor body and is composed of the rotation matrix \mathbf{R} and the position vector \mathbf{p} expressed in successor frame coordinates. The free modes of a joint define the directions in which motion is allowed. They are represented by the $6 \times n_i$ matrix Φ_i whose columns are the Plücker coordinates of the allowable motion. This matrix relates the spatial velocity vector across the joint \mathbf{v}_{rel} to the joint velocity vector $\dot{\mathbf{q}}$,

$$\mathbf{v}_{rel} = \Phi_i \dot{\mathbf{q}}. \quad (1.40)$$

In contrast, the constrained modes of a joint define the directions in which motion is not allowed. They are represented by the $6 \times (6 - n_i)$ matrix Φ_i^c that is complementary to Φ_i . Tables 1.5 and 1.6 contain the formulas of the joint models for all of the joints described in this section. They are used extensively for the dynamic analysis presented in Chapter 2 Dynamics. Additional information on joints can be found in Chapter 3 Mechanisms and Actuation.

1.3.1 Lower Pair Joints

Lower pair joints are mechanically attractive since wear is spread over the whole surface and lubricant is trapped in the small clearance space (in non-idealized systems) between the surfaces, resulting in relatively good lubrication. As can be proved [54] from the requirement for surface contact, there are only six possible forms of lower pair: revolute, prismatic, helical, cylindrical, spherical, and planar joints.

Revolute

The most general form of a revolute joint, often abbreviated as "R" and sometimes referred to colloquially as a

hinge or pin joint, is a lower pair composed of two congruent surfaces of revolution. The surfaces are the same except one of them is an external surface, convex in any plane normal to the axis of revolution, and one is an internal surface, concave in any plane normal to the axis. The surfaces may not be solely in the form of right circular cylinders, since surfaces of that form do not provide any constraint on axial sliding. A revolute joint permits only rotation of one of the bodies joined relative to the other. The position of one body relative to the other may be expressed as the angle between two lines normal to the joint axis, one fixed in each body. Thus, the joint has one degree of freedom (DOF). When the $\hat{\mathbf{z}}$ axis of coordinate frame i is aligned with a revolute joint axis, the formulas in Table 1.5 define the revolute joint model.

Prismatic

The most general form of a prismatic joint, often abbreviated as "P" and sometimes referred to colloquially as a sliding joint, is a lower pair formed from two congruent general cylindrical surfaces. These may not be right circular cylindrical surfaces. A general cylindrical surface is obtained by extruding any curve in a constant direction. Again, one surface is internal and the other is an external surface. A prismatic joint permits only sliding of one of the members joined relative to the other along the direction of extrusion. The position of one body relative to the other is determined by the distance between two points on a line parallel to the direction of sliding, with one point fixed in each body. Thus, this joint also has one degree of freedom. When the $\hat{\mathbf{z}}$ axis of coordinate frame i is aligned with a prismatic joint axis, the formulas in Table 1.5 define the prismatic joint model.

Helical

The most general form of a helical joint, often abbreviated as "H" and sometimes referred to colloquially as a screw joint, is a lower pair formed from two helicoidal surfaces formed by extruding any curve along a helical path. The simple example is a screw and nut wherein the basic generating curve is a pair of straight lines. The angle of rotation about the axis of the screw joint θ is directly related to the distance of displacement of one body relative to the other along that axis d by the expression $d = h\theta$, where the constant h is called the pitch of the screw. When the $\hat{\mathbf{z}}$ axis of coordinate frame i is aligned with a helical joint axis, the formulas in Table 1.5 define the helical joint model.

Joint Type	Joint Transform \mathbf{R}	\mathbf{p}	Free Modes Φ_i	Constrained Modes Φ_i^c	Pose State Vars.	\dot{q}_i
Revolute R	$\begin{bmatrix} c\theta_i & -s\theta_i & 0 \\ s\theta_i & c\theta_i & 0 \\ 0 & 0 & 1 \end{bmatrix}$	$\begin{bmatrix} 0 \\ 0 \\ 0 \end{bmatrix}$	$\begin{bmatrix} 0 \\ 0 \\ 1 \\ 0 \\ 0 \\ 0 \end{bmatrix}$	$\begin{bmatrix} 1 & 0 & 0 & 0 & 0 \\ 0 & 1 & 0 & 0 & 0 \\ 0 & 0 & 0 & 0 & 0 \\ 0 & 0 & 1 & 0 & 0 \\ 0 & 0 & 0 & 1 & 0 \\ 0 & 0 & 0 & 0 & 1 \end{bmatrix}$	θ_i	$\dot{\theta}_i$
Prismatic P	$\mathbf{1}_{3 \times 3}$	$\begin{bmatrix} 1 & 0 & 0 \\ 0 & 1 & 0 \\ 0 & 0 & 1 \end{bmatrix}$	$\begin{bmatrix} 0 \\ 0 \\ 0 \\ 0 \\ 0 \\ 1 \end{bmatrix}$	$\begin{bmatrix} 1 & 0 & 0 & 0 & 0 \\ 0 & 1 & 0 & 0 & 0 \\ 0 & 0 & 1 & 0 & 0 \\ 0 & 0 & 0 & 1 & 0 \\ 0 & 0 & 0 & 0 & 1 \\ 0 & 0 & 0 & 0 & 0 \end{bmatrix}$	d_i	\dot{d}_i
Helical H (pitch h)	$\begin{bmatrix} c\theta_i & -s\theta_i & 0 \\ s\theta_i & c\theta_i & 0 \\ 0 & 0 & 1 \end{bmatrix}$	$\begin{bmatrix} 0 \\ 0 \\ h\theta_i \end{bmatrix}$	$\begin{bmatrix} 0 \\ 0 \\ 1 \\ 0 \\ 0 \\ h \end{bmatrix}$	$\begin{bmatrix} 1 & 0 & 0 & 0 & 0 \\ 0 & 1 & 0 & 0 & 0 \\ 0 & 0 & 0 & 0 & -h \\ 0 & 0 & 1 & 0 & 0 \\ 0 & 0 & 0 & 1 & 0 \\ 0 & 0 & 0 & 0 & 1 \end{bmatrix}$	θ_i	$\dot{\theta}_i$

Table 1.5: Joint model formulas for one-degree-of-freedom lower pair joints, with abbreviations $c\theta_i := \cos\theta_i$ and $s\theta_i := \sin\theta_i$.

Cylindrical

A cylindrical joint, often abbreviated as “C”, is a lower pair formed by contact of two congruent right circular cylinders, one an internal surface and the other an external surface. It permits both rotation about the cylinder axis and sliding parallel to it. Therefore, it is a joint with two degrees of freedom. Lower pair joints with more than one degree of freedom are easily replaced by kinematically equivalent compound joints (see Section 1.3.3) that are serial chains of one-degree-of-freedom lower pairs. In the present case, the cylindrical joint can be replaced by a revolute in series with a prismatic joint whose direction of sliding is parallel to the revolute axis. While simpler to implement using the geometric representation discussed in Section 1.4, this approach has disadvantages for dynamic simulation. Modeling a single cylindrical joint as a combination of a prismatic and revolute joint requires the addition of a virtual link between the two with zero mass and zero length. The massless link can create computa-

tional problems. When the \hat{z} axis of coordinate frame i is aligned with a cylindrical joint axis, the formulas in Table 1.6 define the cylindrical joint model.

Spherical

A spherical joint, often abbreviated as “S”, is a lower pair formed by contact of two congruent spherical surfaces. Once again, one is an internal surface, and the other is an external surface. A spherical joint permits rotation about any line through the center of the sphere. Thus, it permits independent rotation about axes in up to three different directions and has three degrees of freedom. A spherical joint is easily replaced by a kinematically equivalent compound joint consisting of three revolute joints that have concurrent axes. They do not need to be successively orthogonal, but often they are implemented that way. The arrangement is, in general, kinematically equivalent to a spherical joint, but it does exhibit a singularity when the revolute joint axes become coplanar.

This is as compared to the native spherical joint that never has such a singularity. Likewise, if a spherical joint is modeled in simulation as three revolute, computational difficulties again can arise from the necessary inclusion of massless virtual links having zero length. The joint model formulas of a spherical joint are given in Table 1.6.

Planar

A planar joint is formed by planar contacting surfaces. Like the spherical joint, it is a lower pair joint with three degrees of freedom. A kinematically equivalent compound joint consisting of a serial chain of three revolute with parallel axes can replace a planar joint. As was the case with the spherical joint, the compound joint exhibits a singularity when the revolute axes become coplanar. When the \hat{z} axis of coordinate frame i is aligned with the normal to the plane of contact, the formulas in Table 1.6 define the planar joint model.

1.3.2 Higher Pair Joints

Some higher pair joints also have attractive properties, particularly rolling pairs in which one body rolls without slipping over the surface of the other. This is mechanically attractive since the absence of sliding means the absence of abrasive wear. However, since ideal contact occurs at a point, or along a line, application of a load across the joint may lead to very high local stresses resulting in other forms of material failure and, hence, wear. Higher pair joints can be used to create kinematic joints with special geometric properties, as in the case of a gear pair, or a cam and follower pair.

Rolling Contact

Rolling contact actually encompasses several different geometries. Rolling contact in planar motion permits one degree of freedom of relative motion as in the case of a roller bearing, for example. As noted above, rolling contact has desirable wear properties since the absence of sliding means the absence of abrasive wear. Planar rolling contact can take place along a line, thereby spreading the load and wear somewhat. Three-dimensional rolling contact allows rotation about any axis through the point of contact that is, in principle, unique. Hence, a three-dimensional rolling contact pair permits relative motion with three degrees of freedom. When the \hat{z} axis of coordinate frame i is aligned with the axis of rotation and passes through the center of the

roller of fixed radius r , the formulas in Table 1.6 define the planar rolling contact joint model for a roller on a flat surface.

Regardless of whether the joint is planar or three-dimensional, the “no-slip” condition associated with a rolling contact joint requires that the instantaneous relative velocity between the points on the two bodies in contact be zero. If P is the point of rolling contact between bodies i and j ,

$$\mathbf{v}_{P_i/P_j} = 0. \quad (1.41)$$

Likewise, relative acceleration is in the direction of the common normal to the two surfaces at the point of contact. Because the constraint associated with the joint is expressed in terms of velocity, it is nonholonomic, as discussed in Section 1.3.6. A more detailed discussion of the kinematic constraints for rolling contact is found in Section 17.2.2 of Chapter 17 Wheeled Robots.

1.3.3 Compound Joints

Compound kinematic joints are connections between two bodies formed by serial chains of other members and simple kinematic joints. A compound joint may constrain the relative motion of the two bodies joined in the same way as a simple joint. In such a case, the two joints are said to be kinematically equivalent.

Universal

A universal joint, often abbreviated as “U” and referred to as a Cardan or Hooke joint, is a compound joint with two degrees of freedom. It consists of a serial chain of two revolute whose axes intersect orthogonally. The joint model for a universal joint, in which, from Euler angle notation, α_i is the first rotation about the Z -axis and then β_i is the rotation about the Y -axis, is given in Table 1.6. This is the joint for which the matrices Φ_i and Φ_i^c are not constant, so in general, $\dot{\Phi}_i \neq 0$ and $\dot{\Phi}_i^c \neq 0$. In this case, the orientation of the outboard reference frame varies with α_i .

1.3.4 6-DOF Joint

The motion of two bodies not jointed together can be modeled as a six-degree-of-freedom “joint” that introduces no constraints. This is particularly useful for mobile robots, such as aircraft, that make at most intermittent contact with the ground, and thus, a body in

free motion relative to the fixed frame is termed a *floating base*. Such a free motion joint model enables the position and orientation of a floating base in space to be expressed with six joint variables. The 6-DOF joint model is included in Table 1.6.

1.3.5 Physical Realization

In an actual robotic mechanism, the joints may have physical limits beyond which motion is prohibited. The workspace (see Section 1.5) of a robotic manipulator is determined by considering the combined limits and freedom of motion of all of the joints within the mechanism. Revolute joints are easily actuated by rotating motors and are, therefore, extremely common in robotic systems. They may also be present as passive, unactuated joints. Also common, although less so than revolute, prismatic joints are relatively easily actuated by means of linear actuators such as hydraulic or pneumatic cylinders, ball screws, or screw jacks. They always have motion limits since unidirectional sliding can, in principle, produce infinite displacements. Screw joints are most often found in robotic mechanisms as constituents of linear actuators such as screw jacks and ball screws and are seldom used as primary kinematic joints. Joints with more than one degree of freedom are generally used passively in robotic mechanisms because each degree of freedom of an active joint must be separately actuated. Passive spherical joints are quite often found in robotic mechanisms, while passive planar joints are only occasionally found. The effect of an actuated spherical joint is achieved by employing the kinematically equivalent combination of three revolute and actuating each. Universal joints are used in robotic mechanisms in both active and passive forms.

Serial chains are commonly denoted by the abbreviations for the joints they contain in the order in which they appear in the chain. For example, an RPR chain contains three links, the first jointed to the base with a revolute and to the second with a prismatic, while the second and third are jointed together with another revolute. If all of the joints are identical, the notation consists of the number of joints preceding the joint abbreviation, such as 6R for a six-axis serial-chain manipulator containing only revolute joints.

Joints are realized with hardware that is more complex than the idealizations presented in Sections 1.3.1 and 1.3.2. For example, a revolute joint may be achieved with a ball bearing composed of a set of bearing balls trapped between two journals. The balls ideally roll without slip-

ping on the journals, thereby taking advantage of the special properties of rolling contact joints. A prismatic joint may be realized by means of a roller-rail assembly.

1.3.6 Holonomic and Nonholonomic Constraints

With the exception of rolling contact, all of the constraints associated with the joints discussed in the preceding sections can be expressed mathematically by equations containing only the joint position variables. These are called holonomic constraints. The number of equations, and hence the number of constraints, is $6 - n$, where n is the number of degrees of freedom of the joint. The constraints are intrinsically part of the axial joint model.

A nonholonomic constraint is one that cannot be expressed in terms of the position variables alone, but includes the time derivative of one or more of those variables. These constraint equations cannot be integrated to obtain relationships solely between the joint variables. The most common example in robotic systems arises from the use of a wheel or roller that rolls without slipping on another member. Nonholonomic constraints, particularly as they apply to wheeled robots, are discussed in more detail in Chapter 17 Wheeled Robots.

1.3.7 Generalized Coordinates

In a robot manipulator consisting of N bodies, $6N$ coordinates are required to specify the position and orientation of all the bodies relative to a coordinate frame. Since some of those bodies are jointed together, a number of constraint equations will establish relationships between some of these coordinates. In this case, the $6N$ coordinates can be expressed as functions of a smaller set of coordinates \mathbf{q} that are all independent. The coordinates in this set are known as generalized coordinates, and motions associated with these coordinates are consistent with all of the constraints. The joint variables \mathbf{q} of a robot manipulator form a set of generalized coordinates [20, 25].

1.4 Geometric Representation

The geometry of a robotic manipulator is conveniently defined by attaching reference frames to each link. While these frames could be located arbitrarily, it is advantageous both for consistency and computational efficiency to adhere to a convention for locating the frames on the

links. Denavit and Hartenberg [13] introduced the foundational convention that has been adapted in a number of different ways, one of which is the convention introduced by Khalil and Dombre [22] used throughout this handbook. In all of its forms, the convention requires only four rather than six parameters to locate one reference frame relative to another. The four parameters are the link length a_i , the link twist α_i , the joint offset d_i , and the joint angle θ_i . This parsimony is achieved through judicious placement of the reference frame origins and axes such that the \hat{x} axis of one frame both intersects and is perpendicular to the \hat{z} axis of the preceding reference frame. The convention is applicable to manipulators consisting of revolute and prismatic joints, so when multi-degree-of-freedom joints are present, they are modeled as combinations of revolute and prismatic joints, as discussed in Section 1.3.

There are essentially four different forms of the convention for locating reference frames in a robotic mechanism. Each exhibits its own advantages by managing trade-offs of intuitive presentation. In the original Denavit and Hartenberg [13] convention, joint i is located between links i and $i + 1$, so it is on the outboard side of link i . Also, the joint offset d_i and joint angle θ_i are measured along and about the $i - 1$ joint axis, so the subscripts of the joint parameters do not match that of the joint axis. Waldron [55] and Paul [36] modified the labeling of axes in the original convention such that joint i is located between links $i - 1$ and i in order to make it consistent with the base member of a serial chain being member 0. This places joint i at the inboard side of link i and is the convention used in all of the other modified versions. Furthermore, Waldron and Paul addressed the mismatch between subscripts of the joint parameters and joint axes by placing the \hat{z}_i axis along the $i + 1$ joint axis. This, of course, relocates the subscript mismatch to the correspondence between the joint axis and the \hat{z} axis of the reference frame. Craig [11] eliminated all of the subscript mismatches by placing the \hat{z}_i axis along joint i , but at the expense of the homogeneous transform ${}^{i-1}\mathbf{T}_i$ being formed with a mixture of joint parameters with subscript i and link parameters with subscript $i - 1$. Khalil and Dombre [22] introduced another variation similar to Craig's except that it defines the link parameters a_i and α_i along and about the \hat{x}_{i-1} axis. In this case, the homogeneous transform ${}^{i-1}\mathbf{T}_i$ is formed only with parameters with subscript i , and the subscript mismatch is such that a_i and α_i indicate the length and twist of link $i - 1$ rather than link i . Thus, in summary, the advantages of the convention used throughout this

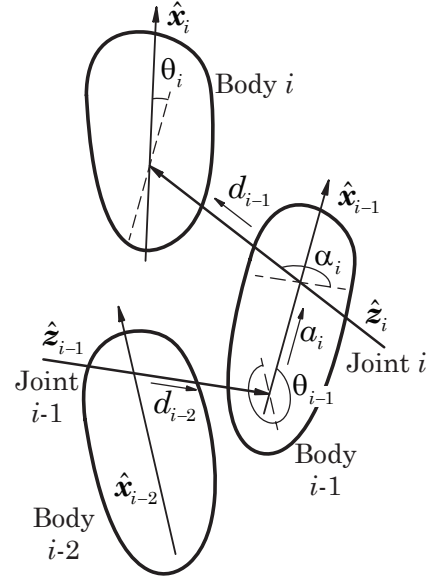


Figure 1.2: Schematic of the numbering of bodies and joints in a robotic manipulator, the convention for attaching reference frames to the bodies, and the definitions of the four parameters, a_i , α_i , d_i , and θ_i , that locate one frame relative to another.

handbook compared to the alternative conventions are that the \hat{z} axes of the reference frames share the common subscript of the joint axes, and the four parameters that define the spatial transform from reference frame i to reference frame $i - 1$ all share the common subscript i .

In this handbook, the convention for serial chain manipulators is shown in Figure 1.2 and summarized as follows. The numbering of bodies and joints follows the convention:

- The N moving bodies of the robotic mechanism are numbered from 1 to N . The number of the base is 0.
- The N joints of the robotic mechanism are numbered from 1 to N , with joint i located between members $i - 1$ and i .

With this numbering scheme, the attachment of reference frames follows the convention:

- The \hat{z}_i axis is located along the axis of joint i .
- The \hat{x}_{i-1} axis is located along the common normal between the \hat{z}_{i-1} and \hat{z}_i axes.

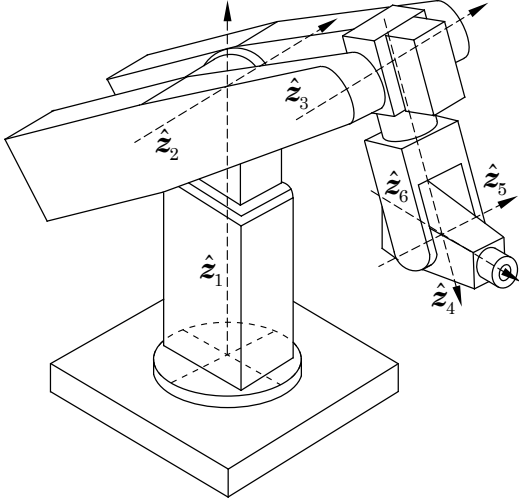


Figure 1.3: Example six-degree-of-freedom serial chain manipulator composed of an articulated arm with no joint offsets and a spherical wrist.

Using the attached frames, the four parameters that locate one frame relative to another are defined as:

- a_i is the distance from \hat{z}_{i-1} to \hat{z}_i along \hat{x}_{i-1} .
- α_i is the angle from \hat{z}_{i-1} to \hat{z}_i about \hat{x}_{i-1} .
- d_i is the distance from \hat{x}_{i-1} to \hat{x}_i along \hat{z}_i .
- θ_i is the angle from \hat{x}_{i-1} to \hat{x}_i about \hat{z}_i .

The geometric parameters for the example manipulator shown in Figure 1.3 are listed in Table 1.7. All of the joints of this manipulator are revolute, and joint 1 has a vertical orientation. Joint 2 is perpendicular to joint 1 and intersects it. Joint 3 is parallel to joint 2, and the length of link 2 is a_3 . Joint 4 is perpendicular to joint 3 and intersects it. Joint 5 likewise intersects joint 4 perpendicularly at an offset of d_4 from joint 3. Finally, joint 6 intersects joint 5 perpendicularly.

With this convention, reference frame i can be located relative to reference frame $i - 1$ by executing a rotation through an angle α_i about the \hat{x}_{i-1} axis, a translation of distance a_i along \hat{x}_{i-1} , a rotation through an angle θ_i about the \hat{z}_i axis, and a translation of distance d_i along \hat{z}_i . Through concatenation of these individual transformations,

$$\mathbf{Rot}(\hat{x}_{i-1}, \alpha_i) \mathbf{Tran}(\hat{x}_{i-1}, a_i) \mathbf{Rot}(\hat{z}_i, \theta_i) \mathbf{Trans}(\hat{z}_i, d_i),$$

the equivalent homogeneous transformation is,

$${}^{i-1}\mathbf{T}_i = \begin{bmatrix} \cos \theta_i & -\sin \theta_i & 0 & a_i \\ \sin \theta_i \cos \alpha_i & \cos \theta_i \cos \alpha_i & -\sin \alpha_i & -\sin \alpha_i d_i \\ \sin \theta_i \sin \alpha_i & \cos \theta_i \sin \alpha_i & \cos \alpha_i & \cos \alpha_i d_i \\ 0 & 0 & 0 & 1 \end{bmatrix}. \quad (1.42)$$

The identification of geometric parameters is addressed in Chapter 14 Model Identification.

1.5 Workspace

Most generally, the workspace of a robotic manipulator is the total volume swept out by the end-effector as the manipulator executes all possible motions. The workspace is determined by the geometry of the manipulator and the limits of the joint motions. It is more specific to define the reachable workspace as the total locus of points at which the end-effector can be placed and the dexterous workspace [56] as the subset of those points at which the end-effector can be placed while having an arbitrary orientation. Dexterous workspaces exist only for certain idealized geometries, so real industrial manipulators with joint motion limits almost never possess dexterous workspaces.

Many serial-chain robotic manipulators are designed such that their joints can be partitioned into a regional structure and an orientation structure. The joints in the regional structure accomplish the positioning of the end-effector in space, and the joints in the orientation structure accomplish the orientation of the end-effector. Typically, the inboard joints of a serial chain manipulator comprise the regional structure, while the outboard joints comprise the orientation structure. Also, since prismatic joints provide no capability for rotation, they are generally not employed within the orientation structure.

The regional workspace volume can be calculated from the known geometry of the serial-chain manipulator and motion limits of the joints. With three inboard joints comprising the regional structure, the area of workspace for the outer two (joints 2 and 3) is computed first, and then the volume is calculated by integrating over the joint variable of the remaining inboard joint (joint 1). In the case of a prismatic joint, this simply involves multiplying the area by the total length of travel of the prismatic joint. In the more common case of a revolute joint, it involves rotating the area about the joint axis through

the full range of motion of the revolute [53]. By the Theorem of Pappus, the associated volume V is

$$V = A\bar{r}\gamma, \quad (1.43)$$

where A is the area, \bar{r} is the distance from the area's centroid to the axis, and γ is the angle through which the area is rotated. The boundaries of the area are determined by tracing the motion of a reference point in the end-effector, typically the center of rotation of the wrist that serves as the orientation structure. Starting with each of the two joints at motion limits and with joint 2 locked, joint 3 is moved until its second motion limit is reached. Joint 3 is then locked, and joint 2 is freed to move to its second motion limit. Joint 2 is again locked, while joint 3 is freed to move back to its original motion limit. Finally, joint 3 is locked, and joint 2 freed to move likewise to its original motion limit. In this way, the trace of the reference point is a closed curve whose area and centroid can be calculated mathematically.

More details on manipulator workspace can be found in Chapter 3 Mechanisms and Actuation and in Chapter 10 Performance Evaluation and Design Criteria.

1.6 Forward Kinematics

The forward kinematics problem for a serial chain manipulator is to find the position and orientation of the end-effector relative to the base given the positions of all of the joints and the values of all of the geometric link parameters. Often, a frame fixed in the end-effector is referred to as the “tool frame”, and while fixed in the final link N , it in general has a constant offset in both position and orientation from frame N . Likewise, a “station frame” is often located in the base to establish the location of the task to be performed. This frame generally has a constant offset in its pose relative to frame 0, which is also fixed in the base.

A more general expression of the forward kinematics problem is to find the relative position and orientation of any two designated members given the geometric structure of the manipulator and the values of a number of joint positions equal to the number of degrees of freedom of the mechanism. The forward kinematics problem is critical for developing manipulator coordination algorithms because joint positions are typically measured by sensors mounted on the joints and it is necessary to calculate the positions of the joint axes relative to the fixed reference frame.

In practice, the forward kinematics problem is solved by calculating the transformation between a reference

frame fixed in the end-effector and another reference frame fixed in the base, i.e. between the tool and station frames. This is straightforward for a serial chain since the transformation describing the position of the end-effector relative to the base is obtained by simply concatenating transformations between frames fixed in adjacent links of the chain. The convention for the geometric representation of a manipulator presented in Section 1.4 reduces this to finding an equivalent 4×4 homogeneous transformation matrix that relates the spatial displacement of the end-effector reference frame to the base reference frame.

For the example serial chain manipulator shown in Figure 1.3 and neglecting the addition of tool and station frames, the transformation is

$${}^0\mathbf{T}_6 = {}^0\mathbf{T}_1 {}^1\mathbf{T}_2 {}^2\mathbf{T}_3 {}^3\mathbf{T}_4 {}^4\mathbf{T}_5 {}^5\mathbf{T}_6. \quad (1.44)$$

Table 1.8 contains the elements of ${}^0\mathbf{T}_6$ that are calculated using Table 1.7 and Equation 1.42.

Once again, homogeneous transformations provide a compact notation, but are computationally inefficient for solving the forward kinematics problem. A reduction in computation can be achieved by separating the position and orientation portions of the transformation to eliminate all multiplications by the 0 and 1 elements of the matrices. In Chapter 2 Dynamics, calculations are made using the spatial vector notation briefly introduced here in Section 1.2.6 and explained in detail in Section 2.2. This approach does not employ homogeneous transformations, but rather separates out the rotation matrices and positions to achieve computation efficiency. Table 2.1 provides the detailed formulas, with the product of spatial transforms particularly relevant to the forward kinematics problem.

Kinematic trees are the general structure of robot mechanisms that do not contain closed loops, and the forward kinematics of tree structures are addressed in Chapter 2 Dynamics. The forward kinematics problem for closed chains is much more complicated because of the additional constraints present. Solution methods for closed chains are included in Chapter 12 Parallel Mechanisms and Robots.

1.7 Inverse Kinematics

The inverse kinematics problem for a serial chain manipulator is to find the values of the joint positions given the position and orientation of the end-effector relative to the base and the values of all of the geometric link

parameters. Once again, this is a simplified statement applying only to serial chains. A more general statement is: Given the relative positions and orientations of two members of a mechanism, find the values of all of the joint positions. This amounts to finding all of the joint positions given the homogeneous transformation between the two members of interest.

In the common case of a six-degree-of-freedom serial chain manipulator, the known transformation is ${}^0\mathbf{T}_6$. Reviewing the formulation of this transformation in Section 1.6, it is clear that the inverse kinematics problem for serial chain manipulators requires the solution of non-linear sets of equations. In the case of a six-degree-of-freedom manipulator, three of these equations relate to the position vector within the homogeneous transform, and the other three relate to the rotation matrix. In the latter case, these three equations cannot come from the same row or column because of the dependency within the rotation matrix. With these non-linear equations, it is possible that no solutions exist or multiple solutions exist. For a solution to exist, the desired position and orientation of the end-effector must lie in the workspace of the manipulator. In cases where solutions do exist, they often cannot be presented in closed form, so numerical methods are required.

1.7.1 Closed-Form Solutions

Closed-form solutions are desirable because they are faster than numerical solutions and readily identify all possible solutions. The disadvantage of closed-form solutions are that they are not general, but robot-dependent. The most effective methods for finding closed-form solutions are ad hoc techniques that take advantage of particular geometric features of specific mechanisms. In general, closed-form solutions can only be obtained for six-degree-of-freedom systems with special kinematic structure characterized by a large number of the geometric parameters defined in Section 1.4 being zero-valued. Most industrial manipulators have such structure because it permits more efficient coordination software. Sufficient conditions for a six-degree-of-freedom manipulator to have closed-form inverse kinematics solutions are [40]: 1) three consecutive revolute joint axes intersect at a common point, as in a spherical wrist; 2) three consecutive revolute joint axes are parallel. Closed-form solution approaches are generally divided into algebraic and geometric methods.

Algebraic Methods

Algebraic methods involve identifying the significant equations containing the joint variables and manipulating them into a soluble form. A common strategy is reduction to a transcendental equation in a single variable such as,

$$C_1 \cos \theta_i + C_2 \sin \theta_i + C_3 = 0, \quad (1.45)$$

where C_1 , C_2 , and C_3 are constants. The solution to such an equation is,

$$\theta_i = 2 \tan^{-1} \left(\frac{C_2 \pm \sqrt{C_2^2 - C_3^2 + C_1^2}}{C_1 - C_3} \right). \quad (1.46)$$

Special cases in which one or more of the constants are zero are also common.

Reduction to a pair of equations having the form,

$$\begin{aligned} C_1 \cos \theta_i + C_2 \sin \theta_i + C_3 &= 0 \\ C_1 \sin \theta_i - C_2 \cos \theta_i + C_4 &= 0, \end{aligned} \quad (1.47)$$

is another particularly useful strategy because only one solution results,

$$\theta_i = \text{Atan2}(-C_1 C_4 - C_2 C_3, C_2 C_4 - C_1 C_3). \quad (1.48)$$

Geometric Methods

Geometric methods involve identifying points on the manipulator relative to which position and/or orientation can be expressed as a function of a reduced set of the joint variables. This often amounts to decomposing the spatial problem into separate planar problems. The resulting equations are solved using algebraic manipulation. The two sufficient conditions for existence of a closed-form solution for a six-degree-of-freedom manipulator that are listed above enable the decomposition of the problem into inverse position kinematics and inverse orientation kinematics. This is the decomposition into regional and orientation structures discussed in Section 1.5, and the solution is found by rewriting Equation 1.44,

$${}^0\mathbf{T}_6 {}^6\mathbf{T}_5 {}^5\mathbf{T}_4 {}^4\mathbf{T}_3 = {}^0\mathbf{T}_1 {}^1\mathbf{T}_2 {}^2\mathbf{T}_3. \quad (1.49)$$

The example manipulator in Figure 1.3 has this structure, and regional structure is commonly known as an articulated or anthropomorphic arm or an elbow manipulator. The solution to the inverse position kinematics problem for such a structure is summarized in Table 1.9. Because there are two solutions for θ_1 and likewise two solutions for both θ_2 and θ_3 corresponding to each

θ_1 solution, there are a total of four solutions to the inverse position kinematics problem of the articulated arm manipulator. The orientation structure is simply a spherical wrist, and the corresponding solution to the inverse orientation kinematics problem is summarized in Table 1.10. Two solutions for θ_5 are given in Table 1.10, but only one solution for both θ_4 and θ_6 corresponds to each. Thus, the inverse orientation kinematics problem of a spherical wrist has two solutions. Combining the regional and orientation structures, the total number of inverse kinematics solutions for the manipulator in Figure 1.3 is eight.

1.7.2 Numerical Methods

Unlike the algebraic and geometric methods used to find closed-form solutions, numerical methods are not robot-dependent, so they can be applied to any kinematic structure. The disadvantages of numerical methods are that they can be slower and in some cases, they do not allow computation of all possible solutions. For a six-degree-of-freedom serial chain manipulator with only revolute and prismatic joints, the translation and rotation equations can always be reduced to a polynomial in a single variable of degree not greater than 16 [27]. Thus, such a manipulator can have as many as sixteen real solutions to the inverse kinematics problem [30]. Since closed form solution of a polynomial equation is only possible if the polynomial is of degree four or less, it follows that many manipulator geometries are not soluble in closed form. In general, a greater number of non-zero geometric parameters corresponds to a polynomial of higher degree in the reduction. For such manipulator structures, the most common numerical methods can be divided into categories of symbolic elimination methods, continuation methods, and iterative methods.

Symbolic Elimination Methods

Symbolic elimination methods involve analytical manipulations to eliminate variables from the system of nonlinear equations to reduce it to a smaller set of equations. Raghavan and Roth [43] used dalytic elimination to reduce the inverse kinematics problem of a general six-revolute serial chain manipulator to a polynomial of degree 16 and to find all possible solutions. The roots provide solutions for one of the joint variables, while the other variables are computed by solving linear systems. Manocha and Canny [29] improved the numerical properties of this technique by reformulating the problem as a

generalized eigenvalue problem. An alternative approach to elimination makes use of Gröbner bases [6, 24].

Continuation Methods

Continuation methods involve tracking a solution path from a start system with known solutions to a target system whose solutions are sought as the start system is transformed into the target system. These techniques have been applied to inverse kinematics problems [51], and special properties of polynomial systems can be exploited to find all possible solutions [58].

Iterative Methods

A number of different iterative methods can be employed to solve the inverse kinematics problem. Most of them converge to a single solution based on an initial guess, so the quality of that guess greatly impacts the solution time. Newton-Raphson methods provide a fundamental approach that uses a first-order approximation to the original equations. Pieper [40] was among the first to apply the method to inverse kinematics, and others have followed [31, 50]. Optimization approaches formulate the problem as a nonlinear optimization problem and employ search techniques to move from an initial guess to a solution [52, 63]. Resolved motion rate control converts the problem to a differential equation [59], and a modified predictor-corrector algorithm can be used to perform the joint velocity integration [7]. Control-theory-based methods cast the differential equation into a control problem [46]. Interval analysis [44] is perhaps one of the most promising iterative methods because it offers rapid convergence to a solution and can be used to find all possible solutions. For complex mechanisms, the damped least squares approach [57] is particularly attractive, and more detail is provided in Chapter 11 Kinematically Redundant Manipulators.

1.8 Forward Instantaneous Kinematics

The forward instantaneous kinematics problem for a serial chain manipulator is: Given the positions of all members of the chain and the rates of motion about all the joints, find the total velocity of the end-effector. Here the rate of motion about the joint is the angular velocity of rotation about a revolute joint or the translational velocity of sliding along a prismatic joint. The total velocity of a member is the velocity of the origin of the reference

frame fixed to it combined with its angular velocity. That is, the total velocity has six independent components and therefore, completely represents the velocity field of the member. It is important to note that this definition includes an assumption that the pose of the mechanism is completely known. In most situations, this means that either the forward or inverse position kinematics problem must be solved before the forward instantaneous kinematics problem can be addressed. The same is true of the inverse instantaneous kinematics problem discussed in the following section. The forward instantaneous kinematics problem is important when doing acceleration analysis for the purpose of studying dynamics. The total velocities of the members are needed for the computation of Coriolis and centripetal acceleration components.

1.8.1 Jacobian

Differentiation with respect to time of the forward position kinematics equations yields a set of equations of the form,

$$\mathbf{v}_N = \mathbf{J}(\mathbf{q})\dot{\mathbf{q}} \quad (1.50)$$

where \mathbf{v}_N is the spatial velocity of the end-effector, $\dot{\mathbf{q}}$ is an N -dimensional vector composed of the joint rates, and $\mathbf{J}(\mathbf{q})$ is a $6 \times N$ matrix whose elements are, in general, non-linear functions of $\mathbf{q}_1, \dots, \mathbf{q}_N$. $\mathbf{J}(\mathbf{q})$ is called the Jacobian matrix of this algebraic system and is expressed relative to the same reference frame as the spatial velocity \mathbf{v}_N . If the joint positions are known, Equation 1.50 yields six linear algebraic equations in the joint rates. If the joint rates are given, solution of Equation 1.50 is a solution of the forward instantaneous kinematics problem. Note that $\mathbf{J}(\mathbf{q})$ can be regarded as a known matrix for this purpose provided all the joint positions are known.

Using the spatial vector notation briefly introduced in Section 1.2.6 and explained in detail in Section 2.2, the Jacobian can be easily computed from the free modes Φ_i of the joints and the associated spatial transforms ${}^j\mathbf{X}_i$. The column(s) of $\mathbf{J}(\mathbf{q})$ associated with joint rate(s) $\dot{\mathbf{q}}_i$ is(are)

$${}^k\mathbf{X}_i\Phi_i,$$

where k denotes any reference frame relative to which \mathbf{v}_N is expressed. Table 1.11 contains an algorithm for efficiently computing the columns of the Jacobian in this manner. Additional information about Jacobians can be found in Chapter 11 Redundant Manipulators.

1.9 Inverse Instantaneous Kinematics

The important problem from the point of view of robotic coordination is the inverse instantaneous kinematics problem. More information on robot coordination can be found in Chapter 5 Motion Planning and Chapter 6 Motion Control. The inverse instantaneous kinematics problem for a serial chain manipulator is: Given the positions of all members of the chain and the total velocity of the end-effector, find the rates of motion of all joints. When controlling a movement of an industrial robot which operates in the point-to-point mode, it is not only necessary to compute the final joint positions needed to assume the desired final hand position. It is also necessary to generate a smooth trajectory for motion between the initial and final positions. There are, of course, an infinite number of possible trajectories for this purpose. However, the most straightforward and successful approach employs algorithms based on the solution of the inverse instantaneous kinematics problem. This technique originated in the work of Whitney [60] and of Pieper [40].

1.9.1 Inverse Jacobian

In order to solve the linear system of equations in the joint rates obtained by decomposing Equation 1.50 into its component equations when \mathbf{v}_N is known, it is necessary to invert the Jacobian matrix. The equation becomes,

$$\dot{\mathbf{q}} = \mathbf{J}^{-1}(\mathbf{q})\mathbf{v}_N \quad (1.51)$$

Since \mathbf{J} is a 6×6 matrix, numerical inversion is not very attractive in real-time software which must run at computation cycle rates of the order of 100 Hz or more. Worse, it is quite possible for \mathbf{J} to become singular ($|\mathbf{J}| = 0$). The inverse does not then exist. More information on singularities can be found in Chapter 3 Mechanisms and Actuation and Chapter 12 Parallel Mechanisms and Robots. Even when the Jacobian matrix does not become singular, it may become ill conditioned, leading to degraded performance in significant portions of the manipulator's workspace. Most industrial robot geometries are simple enough that the Jacobian matrix can be inverted analytically leading to a set of explicit equations for the joint rates. This greatly reduces the number of computation operations needed as compared to numerical inversion. For more complex manipulator geometries, though, numerical inversion is the only solution option.

The Jacobian of a redundant manipulator is not square, so it cannot be inverted. Chapter 11 Kinematically Redundant Manipulators discusses how various pseudoinverses can be used in such cases.

1.10 Static Wrench Transmission

Static wrench analysis of a manipulator establishes the relationship between wrenches applied to the end-effector and forces/torques applied to the joints. This is essential for controlling a manipulator's interactions with its environment. Examples include tasks involving fixed or quasi-fixed workpieces such as inserting a component in place with a specified force and tightening a nut to a prescribed torque. More information can be found in Chapter 7 Force Control and Chapter 27 Contact Modeling and Manipulation. Through the principle of virtual work, the relationship between wrenches applied to the end-effector and forces/torques applied to the joints can be shown to be

$$\boldsymbol{\tau} = \mathbf{J}^T \mathbf{f}, \quad (1.52)$$

where $\boldsymbol{\tau}$ is the n -dimensional vector of applied joint forces/torques for an n -degree-of-freedom manipulator and \mathbf{f} is the spatial force vector

$$\mathbf{f} = \begin{bmatrix} \mathbf{n} \\ \mathbf{f} \end{bmatrix} \quad (1.53)$$

in which \mathbf{n} and \mathbf{f} are the vectors of torques and forces, respectively, applied to the end-effector, both expressed in the reference frame relative to which the Jacobian is also expressed. Thus, in the same way the Jacobian maps the joint rates to the spatial velocity of the end-effector, its transpose maps the wrenches applied to the end-effector to the equivalent joint forces/torques. As in the velocity case, when the Jacobian is not square, the inverse relationship is not uniquely defined.

1.11 Conclusions and Further Reading

This chapter presents an overview of how the fundamentals of kinematics can be applied to robotic mechanisms. The topics include various representations of position and orientation of a rigid body in space, the freedom of motion and accompanying mathematical models of joints, a geometric representation that describes the bodies and joints of a robotics mechanism, the workspace of a manipulator, the problems of forward

and inverse kinematics, the problems of forward and inverse instantaneous kinematics including the definition of the Jacobian, and finally, the transmission of static wrenches. This chapter is certainly not a comprehensive account of robot kinematics. Fortunately, a number of excellent texts provide a broad introduction to robotics with significant focus on kinematics [1, 11, 22, 28, 34, 36, 46, 47, 48, 62].

From a historical perspective, robotics fundamentally changed the nature of the field of mechanism kinematics. Prior to the first work on the generation of coordination equations for robots [40, 60], the focus of the field was almost entirely on single-degree-of-freedom mechanisms. This is why robotics, following on from the advent of digital computing, led to a renaissance of work in mechanism kinematics. More details are found in Chapter 3 Mechanisms and Actuation. The evolution of the field has continued as it has broadened from the study of simple serial chains for industrial robots, the focus of the analysis in this chapter, to parallel machines (see Chapter 12 Parallel Mechanisms and Robots), human-like grippers (see Chapter 15 Robot Hands), robotic vehicles (see Chapter 16 Legged Robots and Chapter 17 Wheeled Robots), and even small-scale robots (see Chapter 18 Micro/Nano Robots).

Rotation Matrix:

$${}^j\mathbf{R}_i = \begin{bmatrix} r_{11} & r_{12} & r_{13} \\ r_{21} & r_{22} & r_{23} \\ r_{31} & r_{32} & r_{33} \end{bmatrix}$$

Z-Y-X Euler Angles $[\alpha, \beta, \gamma]$:

$$\begin{aligned} \beta &= \text{Atan2} \left(-r_{31}, \sqrt{r_{11}^2 + r_{21}^2} \right) \\ \alpha &= \text{Atan2} \left(\frac{r_{21}}{\cos \beta}, \frac{r_{11}}{\cos \beta} \right) \\ \gamma &= \text{Atan2} \left(\frac{r_{32}}{\cos \beta}, \frac{r_{33}}{\cos \beta} \right) \end{aligned}$$

X-Y-Z Fixed Angles $[\psi, \theta, \phi]$:

$$\begin{aligned} \theta &= \text{Atan2} \left(-r_{31}, \sqrt{r_{11}^2 + r_{21}^2} \right) \\ \psi &= \text{Atan2} \left(\frac{r_{21}}{\cos \theta}, \frac{r_{11}}{\cos \theta} \right) \\ \phi &= \text{Atan2} \left(\frac{r_{32}}{\cos \theta}, \frac{r_{33}}{\cos \theta} \right) \end{aligned}$$

Angle-Axis $\theta \hat{\mathbf{w}}$:

$$\begin{aligned} \theta &= \cos^{-1} \left(\frac{r_{11} + r_{22} + r_{33} - 1}{2} \right) \\ \hat{\mathbf{w}} &= \frac{1}{2 \sin \theta} \begin{bmatrix} r_{32} - r_{23} \\ r_{13} - r_{31} \\ r_{21} - r_{12} \end{bmatrix} \end{aligned}$$

Unit Quaternions $[\epsilon_0 \ \epsilon_1 \ \epsilon_2 \ \epsilon_3]^T$:

$$\begin{aligned} \epsilon_0 &= \frac{1}{2} \sqrt{1 + r_{11} + r_{22} + r_{33}} \\ \epsilon_1 &= \frac{r_{32} - r_{23}}{4\epsilon_0} \\ \epsilon_2 &= \frac{r_{13} - r_{31}}{4\epsilon_0} \\ \epsilon_3 &= \frac{r_{21} - r_{12}}{4\epsilon_0} \end{aligned}$$

Table 1.2: Conversions from a rotation matrix to various representations of orientation.

Angle-Axis $\theta \hat{\mathbf{w}}$ to Unit Quaternion $[\epsilon_0 \ \epsilon_1 \ \epsilon_2 \ \epsilon_3]^T$

$$\begin{aligned} \epsilon_0 &= \cos \frac{\theta}{2} \\ \epsilon_1 &= w_x \sin \frac{\theta}{2} \\ \epsilon_2 &= w_y \sin \frac{\theta}{2} \\ \epsilon_3 &= w_z \sin \frac{\theta}{2} \end{aligned}$$

Unit Quaternion $[\epsilon_0 \ \epsilon_1 \ \epsilon_2 \ \epsilon_3]^T$ to Angle-Axis $\theta \hat{\mathbf{w}}$:

$$\begin{aligned} \theta &= 2 \cos^{-1} \epsilon_0 \\ w_x &= \frac{\epsilon_1}{\sin \frac{\theta}{2}} \\ w_y &= \frac{\epsilon_2}{\sin \frac{\theta}{2}} \\ w_z &= \frac{\epsilon_3}{\sin \frac{\theta}{2}} \end{aligned}$$

Table 1.3: Conversions from angle-axis to unit quaternion representations of orientation and vice versa.

Screw Transformation to Homogeneous Transformation:

$$\begin{aligned} {}^j\mathbf{R}_i &= \\ \begin{bmatrix} w_x^2 v_\theta + c_\theta & w_x w_y v_\theta - w_z s_\theta & w_x w_z v_\theta + w_y s_\theta \\ w_x w_y v_\theta + w_z s_\theta & w_y^2 v_\theta + c_\theta & w_y w_z v_\theta - w_x s_\theta \\ w_x w_z v_\theta - w_y s_\theta & w_y w_z v_\theta + w_x s_\theta & w_z^2 v_\theta + c_\theta \end{bmatrix} \\ {}^j\mathbf{p}_i &= (\mathbf{1}_{3 \times 3} - {}^j\mathbf{R}_i) \boldsymbol{\rho} + h \theta \hat{\mathbf{w}} \end{aligned}$$

Homogeneous Transformation to Screw Transformation:

$$\begin{aligned} \mathbf{l} &= \begin{bmatrix} r_{32} - r_{23} \\ r_{13} - r_{31} \\ r_{21} - r_{12} \end{bmatrix}^T \\ \theta &= \text{sign}(\mathbf{l}^T {}^j\mathbf{p}_i) \left| \cos^{-1} \left(\frac{r_{11} + r_{22} + r_{33} - 1}{2} \right) \right| \\ h &= \frac{\mathbf{l}^T {}^j\mathbf{p}_i}{2\theta \sin \frac{\theta}{2}} \\ \boldsymbol{\rho} &= \frac{(\mathbf{1}_{3 \times 3} - {}^j\mathbf{R}_i^T) {}^j\mathbf{p}_i}{2(1 - \cos \theta)} \\ \hat{\mathbf{w}} &= \frac{\mathbf{l}}{2 \sin \theta} \end{aligned}$$

Table 1.4: Conversions from a screw transformation to a homogeneous transformation and vice versa, with abbreviations $c_\theta := \cos \theta$, $s_\theta := \sin \theta$, and $v_\theta := 1 - \cos \theta$.

i	α_i	a_i	d_i	θ_i
1	0	0	0	θ_1
2	$-\frac{\pi}{2}$	0	0	θ_2
3	0	a_3	0	θ_3
4	$-\frac{\pi}{2}$	0	d_4	θ_4
5	$\frac{\pi}{2}$	0	0	θ_5
6	$-\frac{\pi}{2}$	0	0	θ_6

Table 1.7: Geometric parameters of the example serial chain manipulator in Figure 1.3.

${}^0\mathbf{T}_6 =$	$\begin{bmatrix} r_{11} & r_{12} & r_{13} & {}^0p_6^x \\ r_{21} & r_{22} & r_{23} & {}^0p_6^y \\ r_{31} & r_{32} & r_{33} & {}^0p_6^z \\ 0 & 0 & 0 & 1 \end{bmatrix}$
$r_{11} =$	$c_{\theta_1}(s_{\theta_2}s_{\theta_3} - c_{\theta_2}c_{\theta_3})(s_{\theta_4}s_{\theta_6} - c_{\theta_4}c_{\theta_5}c_{\theta_6})$ $-c_{\theta_1}s_{\theta_5}c_{\theta_6}(c_{\theta_2}s_{\theta_3} + s_{\theta_2}c_{\theta_3})$ $+s_{\theta_1}(s_{\theta_4}c_{\theta_5}c_{\theta_6} + c_{\theta_4}s_{\theta_6})$
$r_{21} =$	$s_{\theta_1}(s_{\theta_2}s_{\theta_3} - c_{\theta_2}c_{\theta_3})(s_{\theta_4}s_{\theta_6} - c_{\theta_4}c_{\theta_5}c_{\theta_6})$ $-s_{\theta_1}s_{\theta_5}c_{\theta_6}(c_{\theta_2}s_{\theta_3} + s_{\theta_2}c_{\theta_3})$ $-c_{\theta_1}(s_{\theta_4}c_{\theta_5}c_{\theta_6} + c_{\theta_4}s_{\theta_6})$
$r_{31} =$	$(c_{\theta_2}s_{\theta_3} + s_{\theta_2}c_{\theta_3})(s_{\theta_4}s_{\theta_6} - c_{\theta_4}c_{\theta_5}c_{\theta_6})$ $+s_{\theta_5}c_{\theta_6}(s_{\theta_2}s_{\theta_3} - c_{\theta_2}c_{\theta_3})$
$r_{12} =$	$c_{\theta_1}(s_{\theta_2}s_{\theta_3} - c_{\theta_2}c_{\theta_3})(c_{\theta_4}c_{\theta_5}s_{\theta_6} + s_{\theta_4}c_{\theta_6})$ $+c_{\theta_1}s_{\theta_5}s_{\theta_6}(c_{\theta_2}s_{\theta_3} + s_{\theta_2}c_{\theta_3})$ $+s_{\theta_1}(c_{\theta_4}c_{\theta_6} - s_{\theta_4}c_{\theta_5}s_{\theta_6})$
$r_{22} =$	$s_{\theta_1}(s_{\theta_2}s_{\theta_3} - c_{\theta_2}c_{\theta_3})(c_{\theta_4}c_{\theta_5}s_{\theta_6} + s_{\theta_4}c_{\theta_6})$ $+s_{\theta_1}s_{\theta_5}s_{\theta_6}(c_{\theta_2}s_{\theta_3} + s_{\theta_2}c_{\theta_3})$ $-c_{\theta_1}(c_{\theta_4}c_{\theta_6} - s_{\theta_4}c_{\theta_5}s_{\theta_6})$
$r_{32} =$	$(c_{\theta_2}s_{\theta_3} + s_{\theta_2}c_{\theta_3})(c_{\theta_4}c_{\theta_5}s_{\theta_6} + s_{\theta_4}c_{\theta_6})$ $-s_{\theta_5}s_{\theta_6}(s_{\theta_2}s_{\theta_3} - c_{\theta_2}c_{\theta_3})$
$r_{13} =$	$c_{\theta_1}c_{\theta_4}s_{\theta_5}(s_{\theta_2}s_{\theta_3} - c_{\theta_2}c_{\theta_3})$ $-c_{\theta_1}c_{\theta_5}(c_{\theta_2}s_{\theta_3} + s_{\theta_2}c_{\theta_3})$ $-s_{\theta_1}s_{\theta_4}s_{\theta_5}$
$r_{23} =$	$s_{\theta_1}c_{\theta_4}s_{\theta_5}(s_{\theta_2}s_{\theta_3} - c_{\theta_2}c_{\theta_3})$ $-s_{\theta_1}c_{\theta_5}(c_{\theta_2}s_{\theta_3} + s_{\theta_2}c_{\theta_3}) + c_{\theta_1}s_{\theta_4}s_{\theta_5}$
$r_{33} =$	$c_{\theta_4}s_{\theta_5}(c_{\theta_2}s_{\theta_3} + s_{\theta_2}c_{\theta_3})$ $+c_{\theta_5}(s_{\theta_2}s_{\theta_3} - c_{\theta_2}c_{\theta_3})$
${}^0p_6^x =$	$a_2c_{\theta_1}c_{\theta_2} - d_4c_{\theta_1}(c_{\theta_2}s_{\theta_3} + s_{\theta_2}c_{\theta_3})$
${}^0p_6^y =$	$a_2s_{\theta_1}c_{\theta_2} - d_4s_{\theta_1}(c_{\theta_2}s_{\theta_3} + s_{\theta_2}c_{\theta_3})$
${}^0p_6^z =$	$-a_2s_{\theta_2} + d_4(s_{\theta_2}s_{\theta_3} - c_{\theta_2}c_{\theta_3})$

Table 1.8: Forward kinematics of the example serial chain manipulator in Figure 1.3, with abbreviations $c_{\theta_i} := \cos \theta_i$ and $s_{\theta_i} := \sin \theta_i$.

$\theta_1 =$	$Atan2({}^0p_6^y, {}^0p_6^x)$ or $Atan2(-{}^0p_6^y, -{}^0p_6^x)$.
$\theta_3 =$	$-Atan2(D, \pm\sqrt{1-D^2})$ where $D := \frac{({}^0p_6^x)^2 + ({}^0p_6^y)^2 + ({}^0p_6^z)^2 - a_3^2 - d_4^2}{2a_3d_4}$
$\theta_2 =$	$Atan2({}^0p_6^z, \sqrt{({}^0p_6^x)^2 + ({}^0p_6^y)^2})$ $-Atan2(d_4 \sin \theta_3, a_3 + d_4 \cos \theta_3)$.

Table 1.9: Inverse position kinematics of the articulated arm within the example serial chain manipulator in Figure 1.3.

$\theta_5 =$	$Atan2(\pm\sqrt{1 - (r_{13}s_{\theta_1} - r_{23}c_{\theta_1})^2}, r_{13}s_{\theta_1} - r_{23}c_{\theta_1})$
$\theta_4 =$	$Atan2(\mp(r_{13}c_{\theta_1} + r_{23}s_{\theta_1})s_{(\theta_2+\theta_3)} \mp r_{33}c_{(\theta_2+\theta_3)}, \pm(r_{13}c_{\theta_1} + r_{23}s_{\theta_1})c_{(\theta_2+\theta_3)} \mp r_{23}s_{(\theta_2+\theta_3)})$
$\theta_6 =$	$Atan2(\pm(r_{12}s_{\theta_1} + r_{22}c_{\theta_1}) \pm (r_{11}s_{\theta_1} - r_{21}c_{\theta_1}))$

where the \pm choice for θ_5 dictates all of the subsequent \pm and \mp for θ_4 and θ_6 .

Table 1.10: Inverse orientation kinematics of the spherical wrist within the example serial chain manipulator in Figure 1.3, with abbreviations $c_{\theta_i} := \cos \theta_i$ and $s_{\theta_i} := \sin \theta_i$.

n_i	number of degrees of freedom of joint i
\mathbf{J}	${}^k\mathbf{v}_N = \mathbf{J}(\mathbf{q})\dot{\mathbf{q}}$, where k is any frame
\mathbf{J}_{n_i}	n_i column(s) of \mathbf{J} associated with $\dot{\mathbf{q}}_i$
Φ_ω	first 3 rows of Φ
Φ_v	last 3 rows of Φ

$$\mathbf{J}_{n_i} = {}^k\mathbf{X}_i\Phi_i$$

expression	computed value
$\mathbf{X}_1\mathbf{X}_2$	$(\mathbf{R}_1\mathbf{R}_2; \mathbf{p}_2 + \mathbf{R}_2^T\mathbf{p}_1)$
$\mathbf{X}\Phi$	$(\mathbf{R}\Phi_\omega; \mathbf{R}(\Phi_v - \mathbf{p} \times \Phi_\omega))$
\mathbf{X}^{-1}	$(\mathbf{R}^T; -\mathbf{R}\mathbf{p})$
$\mathbf{X}^{-1}\Phi$	$(\mathbf{R}^T\Phi_\omega; \mathbf{R}^T\Phi_v + \mathbf{p} \times \mathbf{R}^T\Phi_\omega)$

Table 1.11: Algorithm for computing the columns of the Jacobian from the free modes of the joints.

Joint Type	Joint Transform		Free Modes Φ_i	Constrained Modes Φ_i^c	Pose Vars.	Vel. Vars. \dot{q}_i
	R	p				
Cylindrical C	$\begin{bmatrix} c_{\theta_i} & -s_{\theta_i} & 0 \\ s_{\theta_i} & c_{\theta_i} & 0 \\ 0 & 0 & 1 \end{bmatrix}$	$\begin{bmatrix} 0 \\ 0 \\ d_i \end{bmatrix}$	$\begin{bmatrix} 0 & 0 \\ 0 & 0 \\ 1 & 0 \\ 0 & 0 \\ 0 & 0 \\ 0 & 1 \end{bmatrix}$	$\begin{bmatrix} 1 & 0 & 0 & 0 \\ 0 & 1 & 0 & 0 \\ 0 & 0 & 0 & 0 \\ 0 & 0 & 1 & 0 \\ 0 & 0 & 0 & 1 \\ 0 & 0 & 0 & 0 \end{bmatrix}$	θ_i d_i	$\begin{bmatrix} \dot{\theta}_i \\ \dot{d}_i \end{bmatrix}$
Spherical* S	$\begin{bmatrix} \text{see} \\ \text{Table 1.1} \end{bmatrix}$	$\begin{bmatrix} 0 \\ 0 \\ 0 \end{bmatrix}$	$\begin{bmatrix} 1 & 0 & 0 \\ 0 & 1 & 0 \\ 0 & 0 & 1 \\ 0 & 0 & 0 \\ 0 & 0 & 0 \\ 0 & 0 & 0 \end{bmatrix}$	$\begin{bmatrix} 0 & 0 & 0 \\ 0 & 0 & 0 \\ 0 & 0 & 0 \\ 1 & 0 & 0 \\ 0 & 1 & 0 \\ 0 & 0 & 1 \end{bmatrix}$	ϵ_i	$\omega_i \text{ rel}$
Planar	$\begin{bmatrix} c_{\theta_i} & -s_{\theta_i} & 0 \\ s_{\theta_i} & c_{\theta_i} & 0 \\ 0 & 0 & 1 \end{bmatrix}$	$\begin{bmatrix} c_{\theta_i} d_{xi} - s_{\theta_i} d_{yi} \\ s_{\theta_i} d_{xi} + c_{\theta_i} d_{yi} \\ 0 \end{bmatrix}$	$\begin{bmatrix} 0 & 0 & 0 \\ 0 & 0 & 0 \\ 1 & 0 & 0 \\ 0 & 1 & 0 \\ 0 & 0 & 1 \\ 0 & 0 & 0 \end{bmatrix}$	$\begin{bmatrix} 1 & 0 & 0 \\ 0 & 1 & 0 \\ 0 & 0 & 0 \\ 0 & 0 & 0 \\ 0 & 0 & 0 \\ 0 & 0 & 1 \end{bmatrix}$	θ_i d_{xi} d_{yi}	$\begin{bmatrix} \dot{\theta}_i \\ \dot{d}_{xi} \\ \dot{d}_{yi} \end{bmatrix}$
Flat Planar Rolling Contact (fixed radius r)	$\begin{bmatrix} c_{\theta_i} & -s_{\theta_i} & 0 \\ s_{\theta_i} & c_{\theta_i} & 0 \\ 0 & 0 & 1 \end{bmatrix}$	$\begin{bmatrix} r\theta_i c_{\theta_i} - r s_{\theta_i} \\ -r\theta_i s_{\theta_i} - r c_{\theta_i} \\ 0 \end{bmatrix}$	$\begin{bmatrix} 0 \\ 0 \\ 1 \\ r \\ 0 \\ 0 \end{bmatrix}$	$\begin{bmatrix} 1 & 0 & 0 & 0 & 0 \\ 0 & 1 & 0 & 0 & 0 \\ 0 & 0 & -r & 0 & 0 \\ 0 & 0 & 1 & 0 & 0 \\ 0 & 0 & 0 & 1 & 0 \\ 0 & 0 & 0 & 0 & 1 \end{bmatrix}$	θ_i	$\dot{\theta}_i$
Universal U	$\begin{bmatrix} c_{\alpha_i} c_{\beta_i} & -s_{\alpha_i} & c_{\alpha_i} s_{\beta_i} \\ s_{\alpha_i} c_{\beta_i} & c_{\alpha_i} & s_{\alpha_i} s_{\beta_i} \\ -s_{\beta_i} & 0 & c_{\beta_i} \end{bmatrix}$	$\begin{bmatrix} 0 \\ 0 \\ 0 \end{bmatrix}$	$\begin{bmatrix} -s_{\beta_i} & 0 \\ 0 & 1 \\ c_{\beta_i} & 0 \\ 0 & 0 \\ 0 & 0 \\ 0 & 0 \end{bmatrix}$	$\begin{bmatrix} c_{\beta_i} & 0 & 0 & 0 \\ 0 & 0 & 0 & 0 \\ s_{\beta_i} & 0 & 0 & 0 \\ 0 & 1 & 0 & 0 \\ 0 & 0 & 1 & 0 \\ 0 & 0 & 0 & 1 \end{bmatrix}$	α_i β_i	$\begin{bmatrix} \dot{\alpha}_i \\ \dot{\beta}_i \end{bmatrix}$
6-DOF*	$\begin{bmatrix} \text{see} \\ \text{Table 1.1} \end{bmatrix}$	$R^{-1}[{}^0p_i]$	$\mathbf{1}_{6 \times 6}$		ϵ_i 0p_i	$\begin{bmatrix} \omega_i \\ v_i \end{bmatrix}$

Table 1.6: Joint model formulas for higher-degree-of-freedom lower pair joints, universal joint, rolling contact joint, and 6-DOF joint, with abbreviations $c_{\theta_i} := \cos \theta_i$ and $s_{\theta_i} := \sin \theta_i$. *The Euler angles α_i , β_i , and γ_i could be used in place of the unit quaternion ϵ_i to represent orientation.

Bibliography

- [1] H. Asada and J.-J. E. Slotine, *Robot Analysis and Control*, New York: John Wiley & Sons, 1986.
- [2] J. E. Baker and I. A. Parkin, *Fundamentals of Screw Motion: Seminal Papers by Michel Chasles and Olinde Rodrigues*, translated from O. Rodrigues, “Des lois géométriques qui régissent les déplacements d’un système dans l’espace,” *Journal de Mathématiques Pures et Appliquées de Liouville*, vol. 5, pp. 380–440, 1840. Translation published by School of Information Technologies, The University of Sydney, 2003.
- [3] J. E. Baker and K. Wohlhart, *Motor Calculus*, translated from R. von Mises, “Motorrechnung, ein neues Hilfsmittel in der Mechanik,” *Zeitschrift für Angewandte Mathematik und Mechanik*, Band 2, Heft 2, S. 155–181, 1924; and “Anwendungen der Motorrechnung,” *ibid* Band 4, Heft 3, S. 193–213, 1924. Translation published by the Institute for Mechanics, T. U. Graz, 1996.
- [4] R. S. Ball, *A Treatise on the Theory of Screws*, Cambridge: Cambridge University Press, 1998.
- [5] O. Bottema and B. Roth, *Theoretical Kinematics*, New York: Dover Publications, 1990.
- [6] B. Buchberger, “Applications of Grobner Basis in Non-Linear Computational Geometry,” *Trends in Computer Algebra. Lecture Notes in Computer Science*, vol. 296, Springer Verlag, 1989.
- [7] H. Cheng and K. Gupta, “A Study of Robot Inverse Kinematics Based Upon the Solution of Differential Equations,” *Journal of Robotic Systems*, vol. 8, no. 2, pp. 115–175, 1991.
- [8] G. S. Chirikjian, “Rigid-Body Kinematics,” *Robotics and Automation Handbook*, Ed. T. Kurfess, London: CRC Press, 2005.
- [9] G. S. Chirikjian and A. B. Kyatkin, *Engineering Applications of Noncommutative Harmonic Analysis*, Boca Raton, Florida: CRC Press, 2001.
- [10] W. K. Clifford, “Preliminary Sketch of Bi-Quaternions,” *Proceedings of the London Mathematical Society*, vol. 4, pp. 381–395, 1873.
- [11] J. J. Craig, *Introduction to Robotics: Mechanics and Control*, Reading, MA: Addison-Wesley, 1986.
- [12] J. K. Davidson and K. H. Hunt, *Robots and Screw Theory: Applications of Kinematics and Statics to Robotics*, Oxford: Oxford University Press, 2004.
- [13] J. Denavit and R. S. Hartenberg, “A Kinematic Notation for Lower-Pair Mechanisms Based on Matrices,” *Journal of Applied Mechanics*, vol. 22, pp. 215–221, 1955.
- [14] J. Duffy, *Analysis of Mechanisms and Robot Manipulators*, New York: Wiley, 1980.
- [15] J. D. Everett, “On a New Method in Statics and Kinematics,” *Messenger of Mathematics*, vol. 45, pp. 36–37, 1875.
- [16] K. S. Fu, R. C. Gonzalez, and C. S. G. Lee, *Robotics: Control, Sensing, Vision, and Intelligence*, New York: McGraw-Hill, 1987.
- [17] H. Grassman, *Die Wissenschaft der extensiven Grösse oder die Ausdehnungslehre*, Leipzig: Verlag von Otto Wigand, 1844.
- [18] W. R. Hamilton, “On Quaternions, or on a New System of Imaginaries in Algebra,” *Philosophical Magazine*, 18 installments July 1844 - April 1850. Edited by D. E. Wilkins, 2000.
- [19] K. H. Hunt, *Kinematic Geometry of Mechanisms*, Oxford: Clarendon Press, 1978.
- [20] T. R. Kane and D. A. Levinson, *Dynamics, Theory and Applications*, New York: McGraw-Hill, 1985.
- [21] A. Karger and J. Novak, *Space Kinematics and Lie Groups*, New York: Routledge, 1985.
- [22] W. Khalil and E. Dombre, *Modeling, Identification and Control of Robots*, New York: Taylor & Francis, 2002.
- [23] A. P. Kotelnikov, “Screw Calculus and Some Applications to Geometry and Mechanics,” *Annals of the Imperial University of Kazan*, 1895.

- [24] P. Kovacs, "Minimum Degree Solutions for the Inverse Kinematics Problem by Application of the Buchberger Algorithm," *Advances in Robot Kinematics*, S. Stifter and J. Lenarcic Eds., Springer Verlag, pp. 326–334, 1991.
- [25] J. L. Lagrange, *Oeuvres de Lagrange*, Paris: Gauthier-Villars, 1773.
- [26] C. S. G. Lee, "Robot Arm Kinematics, Dynamics, and Control," *Computer*, vol. 15, no. 12, pp. 62–80, 1982.
- [27] H. Y. Lee and C. G. Liang, "A New Vector Theory for the Analysis of Spatial Mechanisms," *Mechanisms and Machine Theory*, vol. 23, no. 3, pp. 209–217, 1988.
- [28] F. L. Lewis, C. T. Abdallah, and D. M. Dawson, *Control of Robot Manipulators*, New York: Macmillan, 1993.
- [29] D. Manocha and J. Canny, *Real Time Inverse Kinematics for General 6R Manipulators*, Technical report, University of California, Berkeley, 1992.
- [30] R. Manseur and K. L. Doty, "A Robot Manipulator with 16 Real Inverse Kinematic Solutions," *International Journal of Robotics Research*, vol. 8, no. 5, pp. 75–79, 1989.
- [31] R. Manseur and K. L. Doty, "Fast Inverse Kinematics of 5-Revolute-Axis Robot Manipulators," *Mechanisms and Machine Theory*, vol. 27, no. 5, pp. 587–597, 1992.
- [32] M. T. Mason, *Mechanics of Robotic Manipulation*, Cambridge, MA: MIT Press, 2001.
- [33] J. M. McCarthy, *Introduction to Theoretical Kinematics*, Cambridge, MA: MIT Press, 1990.
- [34] R. M. Murray, Z. Li, and S. S. Sastry, *A Mathematical Introduction to Robotic Manipulation*, Boca Raton, FL: CRC Press, 1994.
- [35] D. E. Orin and W. W. Schrader, "Efficient Computation of the Jacobian for Robot Manipulators," *International Journal of Robotics Research*, vol. 3, no. 4, pp. 66–75, 1984.
- [36] R. Paul, *Robot Manipulators: Mathematics, Programming and Control*, Cambridge, MA: MIT Press, 1982.
- [37] R. P. Paul, B. E. Shimano, and G. Mayer, "Kinematic Control Equations for Simple Manipulators," *IEEE Transactions on Systems, Man, and Cybernetics*, vol. SMC-11, no. 6, pp. 339–455, 1981.
- [38] R. P. Paul and C. N. Stephenson, "Kinematics of Robot Wrists," *International Journal of Robotics Research*, vol. 20, no. 1, pp. 31–38, 1983.
- [39] R. P. Paul and H. Zhang, "Computationally Efficient Kinematics for Manipulators with Spherical wrists based on the Homogeneous Transformation Representation," *International Journal of Robotics Research*, vol. 5, no. 2, pp. 32–44, 1986.
- [40] D. Pieper, *The Kinematics of Manipulators Under Computer Control*, Doctoral Dissertation, Stanford University, 1968.
- [41] J. R. Phillips, *Freedom in Machinery: Volume 1. Introducing Screw Theory*, Cambridge: Cambridge University Press, 1984.
- [42] J. R. Phillips, *Freedom in Machinery: Volume 2. Screw Theory Exemplified*, Cambridge: Cambridge University Press, 1990.
- [43] M. Raghavan and B. Roth, "Kinematic Analysis of the 6R Manipulator of General Geometry," In *Proceedings of the 5th International Symposium on Robotics Research*, 1990.
- [44] R. S. Rao, A. Asaithambi, and S. K. Agrawal, "Inverse Kinematic Solution of Robot Manipulators Using Interval Analysis," *ASME Journal of Mechanical Design*, vol. 120, no. 1, pp. 147–150, 1998.
- [45] F. Reuleaux, *Kinematics of Machinery* New York: Dover Publications, 1963 (reprint of *Theoretische Kinematik*, 1875, in German).
- [46] L. Sciavicco and B. Siciliano, *Modeling and Control of Robot Manipulators*, London: Springer, 2000.
- [47] R. J. Schilling, *Fundamentals of Robotics: Analysis and Control*, Englewood Cliffs, NJ: Prentice-Hall, 1990.
- [48] M. W. Spong and M. Vidyasagar, *Robot Dynamics and Control*, New York: John Wiley & Sons, 1989.
- [49] E. Study, *Geometrie der Dynamen*, Leipzig: Verlag Teubner, 1901.
- [50] S. C. A. Thomopoulos and R. Y. J. Tam, "An Iterative Solution to the Inverse Kinematics of Robotic Manipulators," *Mechanisms and Machine Theory*, vol. 26, no. 4, pp. 359–373, 1991.
- [51] L. W. Tsai and A. P. Morgan "Solving the Kinematics of the Most General Six- and Five-Degree-of-Freedom Manipulators by Continuation Methods," *ASME Journal of Mechanisms, Transmissions, and Automation in Design*, vol. 107, pp. 189–195, 1985.
- [52] J. J. Uicker, Jr., J. Denavit, and R. S. Hartenberg, "An Interactive Method for the Displacement Analysis of Spatial Mechanisms," *Journal of Applied Mechanics*, vol. 31, pp. 309–314, 1964.

- [53] R. Vijaykumar, K. J. Waldron, and M. J. Tsai, "Geometric Optimization of Manipulator Structures for Working Volume and Dexterity," *International Journal of Robotics Research*, vol. 5, no. 2, pp. 91–103, 1986.
- [54] K. J. Waldron, "A Method of Studying Joint Geometry," *Mechanism and Machine Theory*, vol. 7, pp. 347–353, 1972.
- [55] K. J. Waldron, "A Study of Overconstrained Linkage Geometry by Solution of Closure Equations, Part I: A Method of Study," *Mechanism and Machine Theory*, vol. 8, no. 1, pp. 95–104, 1973.
- [56] K. J. Waldron and A. Kumar, "The Dextrous Workspace," ASME paper No./ 80-DETC-108, *ASME Mechanisms Conference*, Los Angeles, September 20 - October 1, 1980.
- [57] C. W. Wampler, "Manipulator Inverse Kinematic Solutions Based on Vector Formulations and Damped Least Squares Methods," *IEEE Transactions on Systems, Man, and Cybernetics*, vol. 16, pp. 93–101, 1986.
- [58] C. W. Wampler, A. P. Morgan, and A. J. Sommese, "Numerical Continuation Methods for Solving Polynomial Systems Arising in Kinematics," *ASME Journal of Mechanical Design*, vol. 112, pp. 59–68, 1990.
- [59] D. E. Whitney, "Resolved Motion Rate Control of Manipulators and Human Prostheses," *IEEE Transactions on Man-Machine Systems*, vol. 10, pp. 47–63, 1969.
- [60] D. E. Whitney, "The Mathematics of Coordinated Control of Prosthetic Arms and Manipulators," *Journal of Dynamic Systems, Measurement, and Control*, vol. 122, pp. 303–309, 1972.
- [61] E. B. Wilson, *Vector Analysis*, based upon the lectures of J. W. Gibbs, New York: Dover Publications, 1960 (reprint of the second edition published by Charles Scribner's Sons, 1909).
- [62] T. Yoshikawa, *Foundations of Robotics*, Cambridge, MA: MIT Press, 1990.
- [63] J. Zhao and N. Badler, "Inverse Kinematics Positioning Using Nonlinear Programming for Highly Articulated Figures," *Transactions on Computer Graphics*, vol. 13, no. 4, pp. 313–336, 1994.